NAVAL POSTGRADUATE SCHOOL

MONTEREY, CALIFORNIA

THESIS

INVESTIGATING INTERACTIONS BETWEEN A BOX-SHAPED UNMANNED UNDERWATER VEHICLE AND MARINE VEGETATION

by

Gladys Anuat

December 2021

Co-Advisors: Anthony G. Pollman
Joseph Klamo

THIS PAGE INTENTIONALLY LEFT BLANK

REPORT DOCUMENTATION PAGE			Form Approved OMB No. 0704-0188

1. AGENCY USE ONLY *(Leave blank)*	**2. REPORT DATE** December 2021	**3. REPORT TYPE AND DATES COVERED** Master's thesis

4. TITLE AND SUBTITLE
INVESTIGATING INTERACTIONS BETWEEN A BOX-SHAPED UNMANNED UNDERWATER VEHICLE AND MARINE VEGETATION

5. FUNDING NUMBERS

6. AUTHOR(S) Gladys Anuat

7. PERFORMING ORGANIZATION NAME(S) AND ADDRESS(ES)
Naval Postgraduate School
Monterey, CA 93943-5000

8. PERFORMING ORGANIZATION REPORT NUMBER

9. SPONSORING / MONITORING AGENCY NAME(S) AND ADDRESS(ES)
N/A

10. SPONSORING / MONITORING AGENCY REPORT NUMBER

11. SUPPLEMENTARY NOTES The views expressed in this thesis are those of the author and do not reflect the official policy or position of the Department of Defense or the U.S. Government.

12a. DISTRIBUTION / AVAILABILITY STATEMENT
Approved for public release. Distribution is unlimited.

12b. DISTRIBUTION CODE
A

13. ABSTRACT (maximum 200 words)

The DOD relies heavily on UUVs for mine countermeasure missions to provide safe passage for their ships. Unwanted interactions between UUVs and marine vegetation present in littoral areas pose a threat to their mission success. Not much is known about the mechanisms of these interactions. This thesis studies the interactions between a box-shaped UUV and two types of marine vegetation found in littoral regions. The equipment and procedures used closely followed previous work done with a torpedo-shaped UUV. To estimate the vehicle's speed, calibration runs were performed. Experimental runs were done, at different speeds, both with and without the UUV constrained. The runs were conducted in different settings consisting of synthetic giant kelp or eelgrass and different density configurations. The resulting interactions were dependent on the vegetation type, vegetation density, vehicle speed, and vehicle geometry. The synthetic giant kelp caused interactions such as blockage and entanglement with the vehicle's body and propellers. The only adverse interactions caused by the synthetic eelgrass were entanglement with the propellers, but they were severe. The best results were those at lower densities and higher speeds, while higher densities and lower speeds had the worst prognosis. The constrained UUV runs resulted in fewer unwanted interactions. When comparing previous results, the torpedo-shaped UUV had more success at going through the vegetation than the box-shaped UUV.

14. SUBJECT TERMS
UUV, ROV, giant kelp, vehicle geometry, blockage, entanglement, eelgrass, vegetation density, speed

15. NUMBER OF PAGES
95

16. PRICE CODE

17. SECURITY CLASSIFICATION OF REPORT	**18. SECURITY CLASSIFICATION OF THIS PAGE**	**19. SECURITY CLASSIFICATION OF ABSTRACT**	**20. LIMITATION OF ABSTRACT**
Unclassified	Unclassified	Unclassified	UU

NSN 7540-01-280-5500

Standard Form 298 (Rev. 2-89)
Prescribed by ANSI Std. 239-18

THIS PAGE INTENTIONALLY LEFT BLANK

Approved for public release. Distribution is unlimited.

INVESTIGATING INTERACTIONS BETWEEN A BOX-SHAPED UNMANNED UNDERWATER VEHICLE AND MARINE VEGETATION

Gladys Anuat
Lieutenant, United States Navy
BS, Polytechnic University of Puerto Rico, 2011

Submitted in partial fulfillment of the
requirements for the degree of

MASTER OF SCIENCE IN SYSTEMS ENGINEERING

from the

NAVAL POSTGRADUATE SCHOOL
December 2021

Approved by: Anthony G. Pollman
Co-Advisor

Joseph Klamo
Co-Advisor

Oleg A. Yakimenko
Chair, Department of Systems Engineering

THIS PAGE INTENTIONALLY LEFT BLANK

ABSTRACT

The DOD relies heavily on UUVs for mine countermeasure missions to provide safe passage for their ships. Unwanted interactions between UUVs and marine vegetation present in littoral areas pose a threat to their mission success. Not much is known about the mechanisms of these interactions. This thesis studies the interactions between a box-shaped UUV and two types of marine vegetation found in littoral regions. The equipment and procedures used closely followed previous work done with a torpedo-shaped UUV. To estimate the vehicle's speed, calibration runs were performed. Experimental runs were done, at different speeds, both with and without the UUV constrained. The runs were conducted in different settings consisting of synthetic giant kelp or eelgrass and different density configurations. The resulting interactions were dependent on the vegetation type, vegetation density, vehicle speed, and vehicle geometry. The synthetic giant kelp caused interactions such as blockage and entanglement with the vehicle's body and propellers. The only adverse interactions caused by the synthetic eelgrass were entanglement with the propellers, but they were severe. The best results were those at lower densities and higher speeds, while higher densities and lower speeds had the worst prognosis. The constrained UUV runs resulted in fewer unwanted interactions. When comparing previous results, the torpedo-shaped UUV had more success at going through the vegetation than the box-shaped UUV.

THIS PAGE INTENTIONALLY LEFT BLANK

Table of Contents

List of Figures

List of Tables

THIS PAGE INTENTIONALLY LEFT BLANK

List of Acronyms and Abbreviations

AUV	Autonomous Underwater Vehicle
DOD	Department of Defense
DOE	Design of Experiment
DOF	Degrees of Freedom
EOD	Explosive Ordnance Disposal
MUV	Micro Underwater Vehicle
NPS	Naval Postgraduate School
REMUS	Remote Environmental Measuring UnitS
ROV	Remotely Operated Vehicle
USB	Universal Serial Bus
USN	U.S. Navy
UUV	Unmanned Underwater Vehicle

THIS PAGE INTENTIONALLY LEFT BLANK

Executive Summary

The use of mines threatens the safe passage of U.S. vessels through restricted waters, narrow straits, and littoral regions. Unmanned Underwater Vehicles (UUVs) are used by the Department of Defense (DOD) for the mine countermeasure mission to neutralize this threat. Marine vegetation present in these littoral areas can cause unwanted interactions, including entanglement, for the UUV thereby preventing it from successfully completing its mission. Little information exists about the mechanisms and likelihoods of entanglement.

This thesis explores the interactions that occur between a blunt, box-shaped UUV and marine vegetation commonly found in the littoral regions. The focus of the study was the effects of vegetation type and density on the type of interaction that occurred with the UUV. This investigation parallels earlier research on traditional torpedo-shaped UUV entanglement in marine vegetation. The same test fixture and basic procedures were used in this study to support direct comparison and provide further insights into the effects that vehicle geometry plays on vegetation interactions. Calibration runs were performed to estimate UUV speed while attached to the carriage for a given gain setting. Experimental runs were conducted at different speeds using different synthetic marine vegetation types (giant kelp and eelgrass) and densities (single, low, medium and high) for each speed. Three different gain settings, corresponding to three different speeds, were chosen to carry out the restricted movement experimental runs. Separate unrestricted movement runs were conducted at a wider range of vehicle speed and operation direction (forward and astern) to observed unbiased operation of the vehicle.

The results show that there are multiple factors that affect the interactions between a box-shaped UUV and marine vegetation. The vegetation type and density, as well as vehicle speed are some of these factors. Higher vegetation density and lower vehicle speed settings resulted in the worst possible interactions. The number, type and severity of the interactions were different with the runs conducted with synthetic giant kelp and those with synthetic eelgrass. For the giant kelp, negative vehicle interactions included propeller entanglement, body entanglement, and blockage. Most interactions between the synthetic eelgrass and the UUV resulted in severe propeller entanglement, while no body entanglement or blockage was observed. Vehicle movement (restricted versus unrestricted) and the implications for the

number thrusters used for each type of movement are also factors. Unrestricted movement runs resulted in more negative interactions because the lateral thrusters were activated whenever the vehicle attempted to maintain depth. Vehicle geometry (and possibly mass) was also determined to be a factor affecting the interactions between UUVs and marine vegetation. The box-shaped, lower mass UUV had many negative interactions with the giant kelp vegetation, to include blockage, while the higher mass, torpedo-shaped UUV was not affected by it. More work can be done to further investigate the effects of vegetation type, vegetation density, vehicle speed, propulsion type, number of propellers (if applicable), and vehicle mass and geometry on entanglement and other negative interactions. Understanding what factors affect interactions between UUVs and marine vegetation could allow for better mission planning and higher probability of mission success.

Acknowledgments

I would like to thank my thesis advisors, Dr. Klamo and Dr. Pollman, for their time, knowledge, and guidance. This thesis would have never been finished if it were not for their dedicated involvement and much needed assistance, in both the experiment and the writing process. Thank you for steering me in the right direction when things did not go as expected and a new direction was required. I would also like to thank my family, starting with my husband, Eddie, and my daughters Sarah and Elissa. Thank you for your love and support.

THIS PAGE INTENTIONALLY LEFT BLANK

CHAPTER 1:
Introduction

This thesis explores the interactions that occur between a blunt, boxish-shaped Remotely Operated Vehicle (ROV) and marine vegetation commonly found in the littoral regions. The main focus of the study was the effects of vegetation type and density on the type of interaction that occurred with the ROV. This investigation parallels previous work done on traditional torpedo-shaped Unmanned Underwater Vehicle (UUV) entanglement with marine vegetation. The same test fixture and basic procedures that were used previously were also used in this study to support direct comparison and provide further insights into the effects that vehicle geometry plays on vegetation interactions.

1.1 Background and Motivation

Mines are readily available to U.S. adversaries and are relatively inexpensive. The use of mines threatens the safe passage of U.S. vessels through restricted waters, narrow straits, and littoral regions. UUVs are used by the Department of Defense (DOD) for the mine countermeasure mission. Unfortunately, there are many types of seaweed located all over the coastal regions of the world where U.S. Navy (USN) underwater vehicles must operate which can interfere with their operations. Marine vegetation present in littoral areas can cause unwanted interactions, including entanglement, thereby preventing a UUV from successfully completing its mission. Little information exists about the mechanisms and likelihoods of entanglement.

There are many different types of UUVs with different geometries, types of propulsion systems, and different dimensions and weight that can be used for missions in shallow waters. If we can understand and estimate the probability a UUV will be entangled given some conditions, in this case UUV geometry and marine vegetation type and density, we can better prepare and prevent UUVs from getting entangled. The findings of the thesis could be used to aid in UUV selection, and possibly to tailor UUV operating or deployment procedures based on maritime vegetation to reduce the chances of UUV entanglement. Reducing the probability of UUV entanglement would significantly improve the Explosive Ordnance

Disposal (EOD) community's ability to successfully complete their mine countermeasure missions. This would allow USN vessels to safely transit littoral regions in order to complete their own missions.

1.1.1 Macrocystis Pyrifera (Giant Kelp)

Macrocystis Pyrifera, commonly known as giant kelp, can grow to heights greater than 100 feet, and provides a habitat for "thousands of marine species" [1]. Figure 1.1 shows a representative giant kelp bed. Despite its resemblance to grass, giant kelp is not a plant, but is a protist brown alga. Unlike most protists, which are single-celled organisms, "giant kelp is a complex species and is the largest protist in the world" [1].

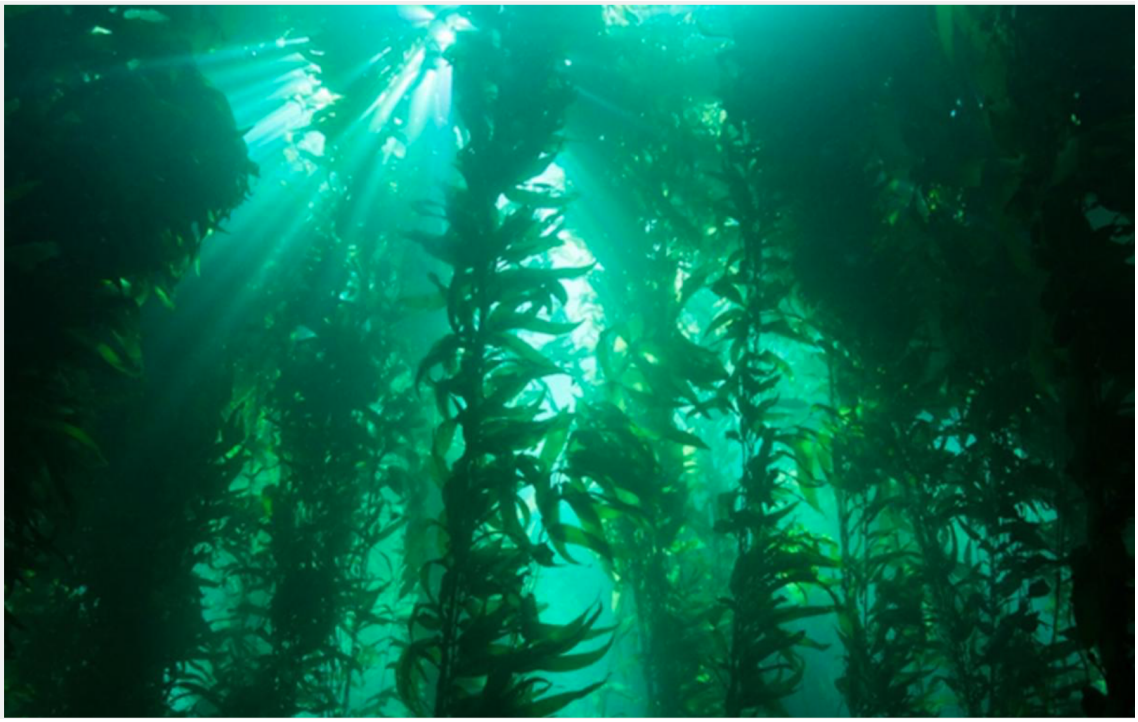

Figure 1.1. Giant Kelp Bed. Photograph showing giant kelp, which is the largest seaweed and the largest marine algae. Source: [1].

Giant kelp does not have roots. Instead, it uses photosynthesis to harvest the sun's energy and gets all its nutrients directly from the water. They grow along rocky coastlines in clear,

nutrient-rich, water with temperatures around 56 to 22 degrees Celsius (42 to 72 degrees Fahrenheit) and where the sunlight can easily penetrate. The amount of dissolved inorganic nitrogen decreases as water temperature increases, negatively impacting the growth of giant kelp [2]. Giant kelp attaches to a "rocky bottom by a structure known as a holdfast" [1]. This species can grow up to two feet a day, being one of the "fastest growing species in the world" [1]. After they reach the surface, giant kelp continues to grow horizontally. A gas-filled pod is present on each of the giant kelp blades. These pods, also referred to as gas bladders or pneumatocysts, help them float and remain upright [1].

Groups of giant kelp can live together, forming a dense kelp forest. Kelp forests are found predominantly on the Pacific Coast, ranging from Alaska all the way south to the waters of Baja California [2]. Giant kelp and bull kelp dominate the kelp forests of the eastern Pacific coast. Figure 1.2 shows, in black, the global giant kelp distribution. The USN operates heavily along the US Pacific coastline where giant kelp are prevalent, from locations such as Naval Base San Diego, Naval Base Coronado, and Naval Station Everett.

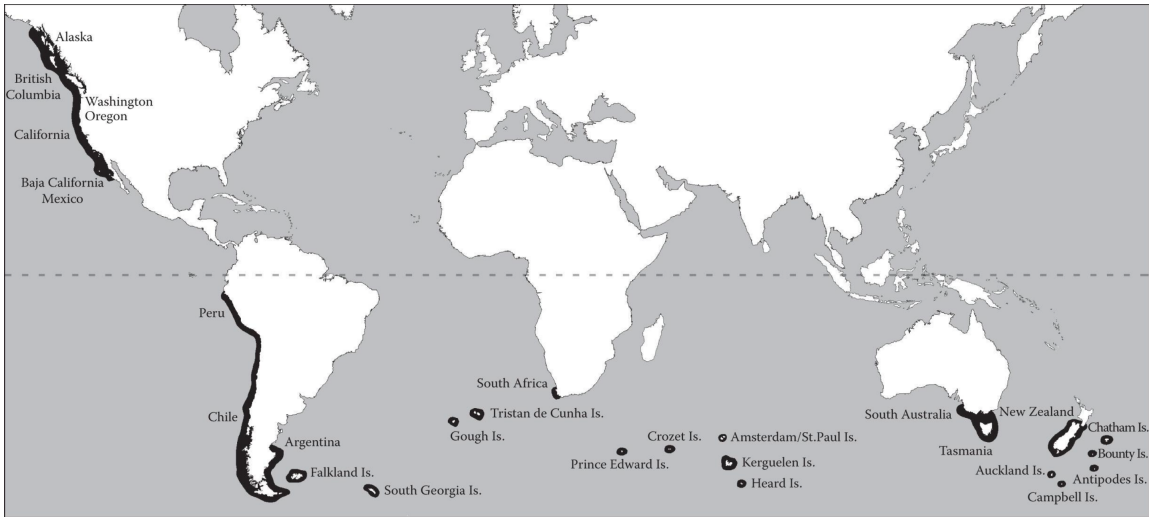

Figure 1.2. Global Giant Kelp Distribution. Map showing global giant kelp distribution, which occur in rocky coastlines with cool and clear water. Source: [3].

1.1.2 Zostera Marina (Eelgrass)

Zostera Marina, commonly known as eelgrass, is the most widely occurring marine angiosperm (flowering plant) in the world [4]. Eelgrass, shown in Figure 1.3, is found in shallow waters of depths ranging all the way from 1 to 15 m. They grow in beds and, similar to other seagrass, their blades are ribbon-like. Depending on the location, the blades can grow up to 1.22 m (4 ft) in length.

Figure 1.3. Eelgrass Bed. Source: [5].

Eelgrass is found in the northern hemisphere, throughout the North Atlantic and North Pacific and in the Mediterranean and Black Seas [5]. Eelgrass can grow in sandy, muddy, or combination of stones, sand or mud sediment. It is found in areas with salinity of 5

to 35 ppt. Figure 1.4 shows, in orange, the locations where eelgrass is found. The USN operates in many of these areas, whose areas of responsibilities are shared between Naval Forces Commands: U.S. Northern Command, U.S. European Command and U.S. Pacific Command [6].

Figure 1.4. Global Eelgrass Distribution. The map illustrates in orange the locations where eelgrass is resident. Source: [5].

1.1.3 Brief Survey of UUVs

UUVs are widely used in the commercial and military communities. UUVs can be divided into ROVs and Autonomous Underwater Vehicles (AUVs) [7]. ROVs need a tether cable for telemetry, control, and sometimes even power, while AUVs do not. As shown in Figure 1.5, most ROVs are box-shaped while most AUVs are torpedo-shaped, although this is not always the case. Commercial ROVs are used for inspection and intervention applications, while commercial AUVs are used for mapping and survey applications [7].

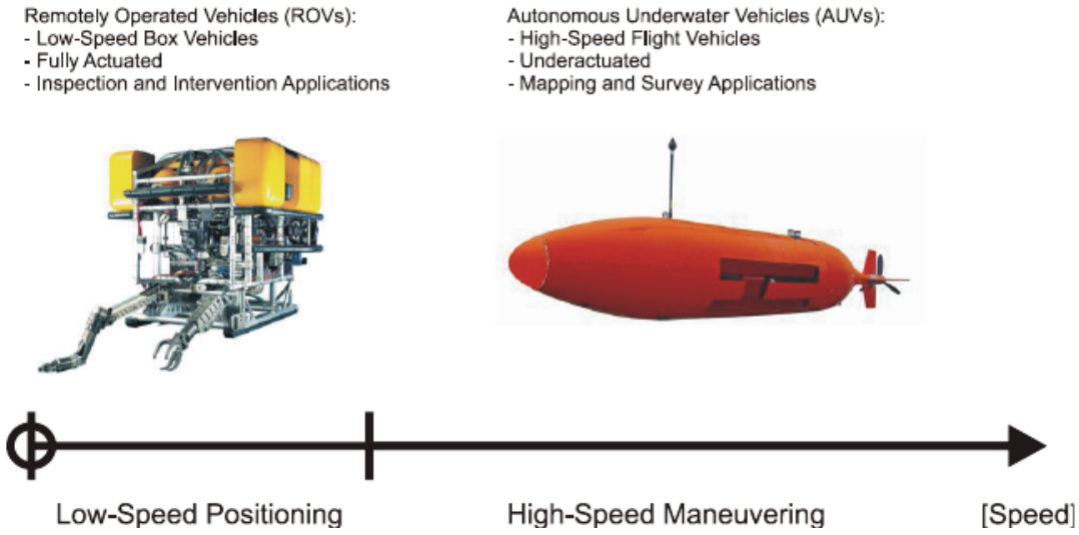

Figure 1.5. Main Differences Between ROVs and AUVs. Image shows the main differences between both types of UUVs involving main geometry, speed, actuation, and commercial applications. Source: [7].

The terms "fully actuated" and "underactuated" refer to the Degrees of Freedom (DOF) control for a vehicle. A ROV can be moved and controlled in all six of its DOF, while an AUV cannot. AUVs need to have enough forward speed so that their control surfaces are able to generate sufficient force and moment on the vehicle to allow for stability and control. On the other hand, an ROV can loiter at a point because its multiple thrusters provide the required control authority. The USN uses ROVs for search and rescue [8], hull inspections, EOD [8], [9], salvaging and other missions requiring the use of cameras or special tools [8]–[10]. Current USN uses for AUVs are battlespace awareness and mine warfare, while future uses include strike capabilities by payload integration [11].

Some UUVs have emerged containing characteristics of both ROVs and AUVs, exploiting the advantages of each. These are called hybrid AUV/ROV [12], [13]. These UUVs can operate with a pre-determined and saved mission, or by user control. They can run both on battery power, when in AUV mode, or on AC power while operating in ROV mode and tethered. Their design allows for both "fully actuated" (6 DOF) and provides reduced low hydrodynamic resistance. Figure 1.6 shows a hybrid AUV/ROV.

Figure 1.6. Hybrid UUV. UUV designed taking advantage of both the ROV and AUV designs. Source: [13].

The most common military use for a UUV is mine warfare. Commercially, UUVs are mostly used in oceanic experiments for data collection. Some UUVs are relatively inexpensive and easy to obtain. Figure 1.7 shows the BlueROV2, which the manufacturer claims is "the world's most affordable high-performance ROV" [14]. This ROV has six T200 thrusters, dimmable lights, a camera, and is commonly used for ocean research and exploration. The vehicle weighs around 97.86 to 106.76 N (22 - 24 lbs) with ballast [14]. Amongst its sensors are a gyroscope, an accelerometer, a magnetometer, an internal barometer, a pressure/depth

and temperature sensor, current and voltage sensor, and a leak detector [14].

Figure 1.7. Blue Robotic's BlueROV2. UUV with box-shaped geometry and six shrouded propellers. Source: [14].

The Remote Environmental Measuring UnitS (REMUS) developed by the Oceanographic Systems Laboratory at the Woods Hole Oceanographic Institution, seen in Figure 1.8, was "one of the most widely used autonomous underwater vehicles in the world" [15] in 2000. Maturation of UUVs and the creation of new UUVs have resulted from improving technologies, continuous engineering development, and experience.

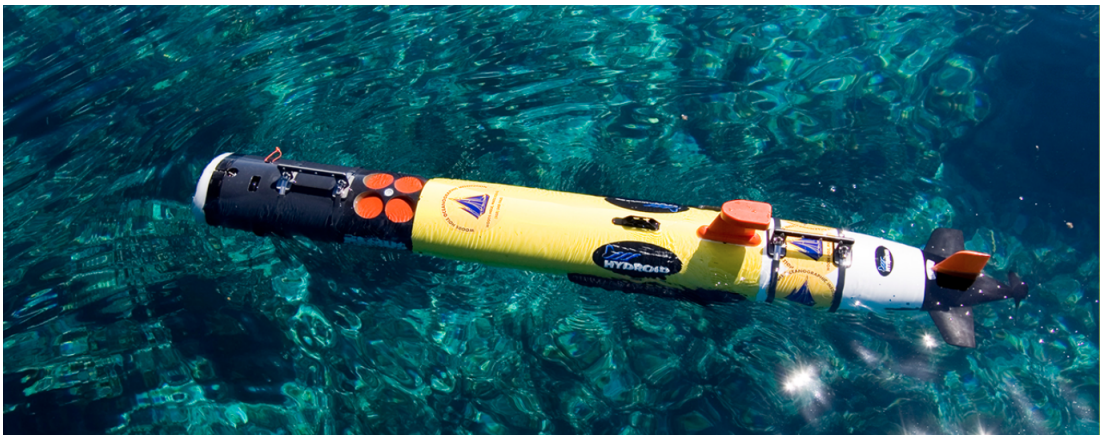

Figure 1.8. Oceanographic Systems Laboratory's REMUS-100. UUV with torpedo shaped geometry and the open three-bladed propeller UUV. Source: [16].

"To improve the performance of UUVs in terms of efficiency and maneuverability, researchers have proposed biomimetic propulsion systems that move using flapping fins rather than rotary propellers" [17]. The use of biomimicry, multiple fins, and improved maneuverability is being used for the Micro Underwater Vehicle (MUV). These types of underwater vehicles have the required size and maneuverability to be used in confined spaces for exploration. Another of these biomimetic UUVs is the BIOSwimmer which was developed by Boston Engineering, and its commercialization started in 2015. The BIOSwimmer, shown in Figure 1.9, is a biologically-inspired UUV. It moves accurately and rapidly, like a fish, and is able to operate in areas that other vehicles are not able to access [18]. "The highly maneuverable UUV performs operations that include inspecting ships, securing ports, and conducting infrastructure searches more rapidly, more accurately, and in more challenging areas than other underwater solutions" [18].

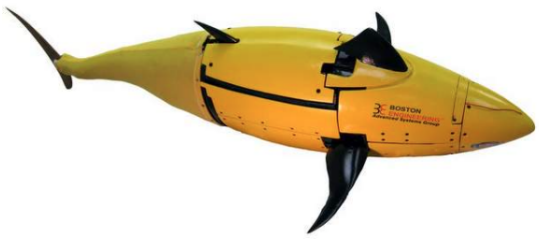

Figure 1.9. Boston Engineering's BIOSwimmer. UUV that has a geometry resembling that of a tuna fish. Source: [18].

NOA MARINE designed an UUV that uses a wave-drive propulsion system that mimics how a squid propels itself [19]. Their design improves the UUV's payload capacity (heavier and bulkier sensors), acoustics, and maneuverability. NOAA MARINE's squid-like UUV, shown in Figure 1.10, will be put to test in the Baltic Sea, conducting a survey. Submarine ground water discharges, seabed integrity, and the nutrient and pollutants within the water will be monitored by NOA MARINE during the survey [19].

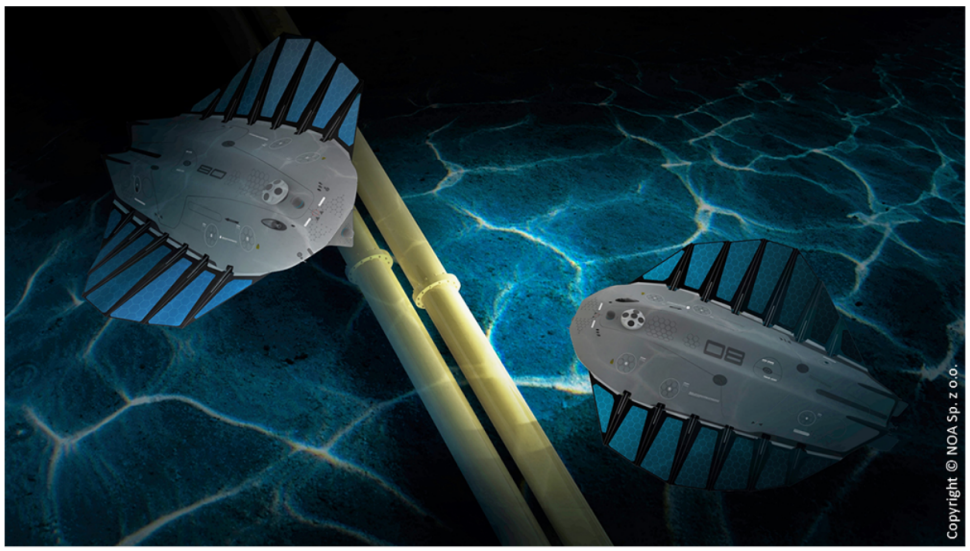

Figure 1.10. NOA MARINE's UUVs. Inspecting a pipe using their wave drive propulsion system, mimicking a squid. Source: [19].

1.2 Previous Work

Currently there is little information regarding the theory of entanglement of marine vegetation on propellers or UUVs, and on the blockage of these vehicles. LCDR Irgens did an "experimental assessment of entanglement for an UUV with an open blade propeller" [20], [21]. A REMUS100 UUV was used to conduct three different entanglement tests with synthetic giant kelp and eelgrass in a tow tank. The first test was "conducted by changing vehicle steady state speed and marine vegetation density" [20], [21]. Another test was "conducted by changing the marine vegetation location relative to the vehicle center-line" [20], [21]. The final test was "conducted by varying the speed of the vehicle when the propeller entered the vegetation field" [20], [21]. The "vegetation density and constant speed entanglement test" [20], [21] showed a higher number of entanglements in eelgrass than giant kelp, in higher vegetation densities than lower ones, and for astern operations than forward operations. The lateral placement test showed a higher number of entanglement events when the vegetation was closer to the propeller, as expected. The accelerating speed entanglement test showed an increase in the likelihood of entanglement as the "ratio of propeller speed to instantaneous vehicle speed" [20], [21], when the propeller entered the vegetation field, increased. The majority of the remaining publicly available work is focused on patent submissions seeking to avoid propeller entanglement.

1.3 Objectives

The main objective of this experimental thesis was to evaluate how encountering different types and densities of marine vegetation affects the operation of a box-shaped UUV. Understanding how the vehicle's geometry and propeller type affects the UUV's interaction with marine vegetation could benefit the DOD when deciding which UUVs to be used for given areas and missions along with guiding the design of future UUVs. Furthermore, by using the same equipment and procedures (with the exception of the UUV itself) from the previous work discussed in Section 1.2, the effects that the vehicle's geometry plays on its probability of entanglement with marine vegetation can begin to be accessed. The marine vegetation chosen for the experiments, giant kelp and eelgrass, are commonly found in littoral waters the USN operates in. The interactions between a box-shaped UUV with six shrouded propellers and different types of marine vegetation were analyzed by changing the vehicle speed and the vegetation type as well as the vegetation density. While there

is very little information on traditional torpedo-shaped UUVs and their interaction with marine vegetation, there is no publicly available information regarding this specific vehicle geometry and propeller type.

1.4 Outline

The layout of this thesis is as follows. This chapter provided the motivation and background information for this thesis. It also provided a brief description of previous related work and the thesis objectives. The equipment used for the experiments is illustrated and discussed in Chapter 2. Chapter 3 goes over the calibration procedures as well as the procedures for the experimental runs. The results are presented and analyzed in Chapter 4 and Chapter 5 is used for future work recommendations.

CHAPTER 2:
Equipment

Chapter 2 provides illustrations and descriptions for the test facility, testing fixture, data acquisition equipment, synthetic marine vegetation, and equipment setup used in this experimental thesis. All of the tools and equipment used in this experiment were the same as the ones used in a previous work [20], [21], with the exception of the UUV itself and UUV interface equipment.

2.1 Test Facility

The water tank utilized for this study is located in Halligan Hall at the Naval Postgraduate School (NPS). The tank is a rectangular basin filled with freshwater and has dimensions of 10.973 m (36') by 0.9144 m (3') by 1.219 m (4') (length x width x depth). Parallel bars on the top of the tank serve as rails for a moving carriage. The carriage is a 1.905 cm (3/4") thick aluminum plate and is mounted on the rails with four bushings that contain self-lubricating ball bearings inside. The bushings have been machined in order to remove a fraction of them and allow unobstructed movement down the tank's full length. The carriage on top of the tow tank is driven by a pulley mechanism powered by a motor. For this experiment, however, it was disconnected from the drive system and the carriage was moved by the thrust of the vehicle. The testing fixture described in Section 2.2 is was used to connect the carriage to the vehicle.

2.2 Testing Fixture

Because the BlueROV2 has six degrees of freedom, as well as a small mass, controlling the vehicle through marine vegetation and having repeatable runs would be impossible; therefore the vehicle was attached to the tank's carriage for a large portion of the test matrix to ensure that the heading and depth remained unchanged throughout the runs. The BlueROV2 was attached to the carriage via a vertical sting and a 3D printed adapter. The sting was 105.41 cm (41.5") by 3.81 cm (1.5") by 2.54 cm (1") (length, width and thickness). It had 30 holes, spaced one inch apart, that allowed for the vehicle to be attached to the

carriage at various depths. The first hole on the sting was centered at 1.27 cm (1/2") from the top of the sting. The sting also had two additional holes on the bottom end to attach to the adapter. The lower hole was centered 2.54 cm (1") from the end of the sting and has 4.445 cm (1.75") center to center from the other adapter attachment hole. The sting was attached to the BlueROV2 using a 3D printed adapter that had dimensions of 22.86 cm (9") by 36.195 cm (14.25") by 13.462 cm (5.3") (length, width and depth). The adapter was made from polycarbonate and 3D printed using a Fortus 400mc printer. Because the BlueROV2 is free-running, the use of a vertical sting and adapter to rigidly hold the UUV at a constant depth along the centerline of the towing tank was necessary to make the runs consistent and repeatable. This removed the possibility of any lateral and vertical movement, as well as pitch, roll and yaw, constraining the vehicle to only forward and aft movement.

The adapter was attached to the BlueROV2 using four #10-32, 1.5-inch screws, four washers and four nuts, tightened using a screwdriver and an open ended wrench. The adapter was attached to the sting using two #10-24, 3-inch screws, two washers and two nuts, and were also tightened using a screwdriver and open-ended wrench. A U-channel is used to provide two attachment points for the vertical sting, using two machined L-brackets. Two screws, four washers and four nuts are used to make this connection and are tightened with screwdriver and open-ended wrench. The top-most point is attached at hole number nine (starting the count at the top of the sting), and the lowest point is attached at hole number 14 (counting from the top of the sting). This attachment location resulted on a vehicle depth of 13.907 ± 2.985 cm (5.475 ± 1.175 in) from the top of the vehicle to the calm water surface or 26.607 ± 2.985 cm (10.475 ± 1.175 in) from its centerline. These values represent depth ranges based on an estimated 5.969 cm (2.35 in) evaporation of the tow tank's water throughout the experiment. Figure 2.1 shows the sting and adapter used during testing. Engineering drawings for the adapter are provided in the Appendix Figure A.1.

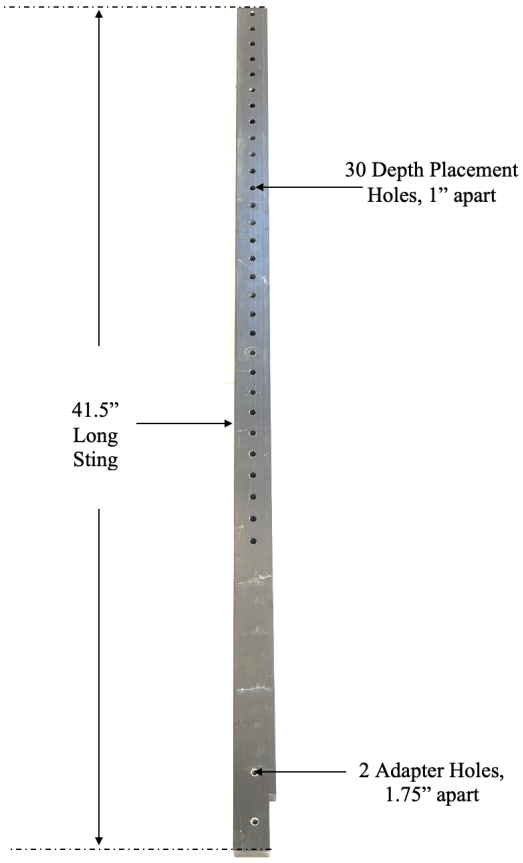

(a) Sting

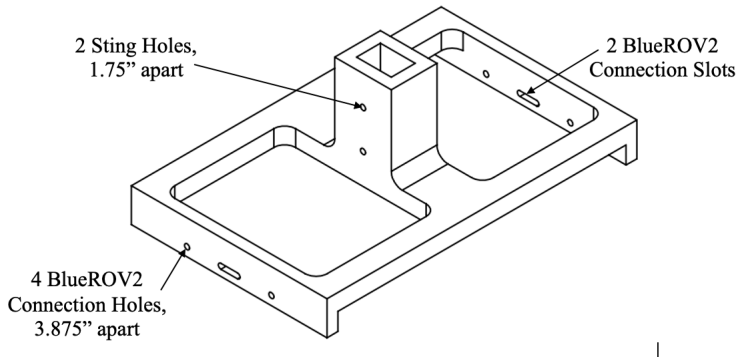

(b) Adapter

Figure 2.1. Sting and Adapter. Image shows the sting and adapter used to physically constrain the motion of the ROV in the tow tank.

.

2.3 Data Acquisition Equipment

A plexiglass plate was used during the calibration runs, and some of the experimental runs, to record the time history of the vehicle position throughout a given run. The plate reflects the ultrasonic pulses produced by the Senix ToughSonic 30 ultrasonic position sensor that is mounted at the end of the tank and aimed at the plate [20]. Figure 2.2 is a photo of the test set-up and includes the ultrasonic position sensor and plexiglass plate. The Senix ToughSonic 30 Ultrasonic Position Sensor was a Model TSPC-15S and was powered at 24 volts by a Keysight E3631 80 Watt DC power supply. The analog voltage output of the sensor was digitized by a National Instruments NI-USB-6363 X-Series Multifunction DAQ and recorded to a laptop using a Universal Serial Bus (USB) connection [20].

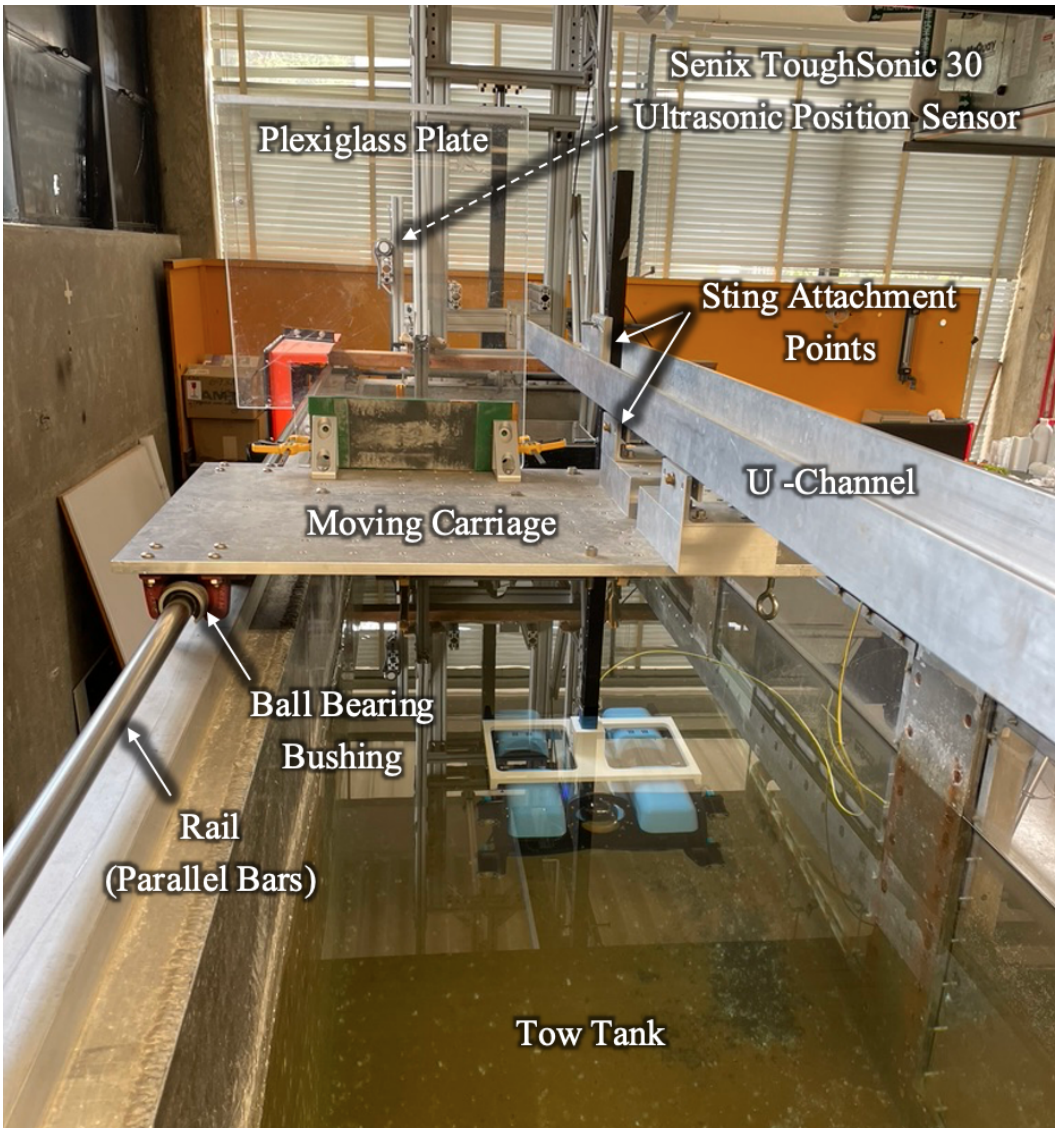

Figure 2.2. Test Facility, Testing Fixture and Part of the Data Acquisition Equipment.

2.4 BlueROV2 Setup

The UUV used in this experiment was the BlueROV2 produced by BlueRobotics. The vehicle, and the software required to operate the vehicle, was setup according to the instructions on the BlueRobotics web-page. The UUV was connected via a 100 m Fathom UUV tether cable to a Fathom-X board. The board was then connected to a laptop via Ethernet cable

and USB. QGroundControl was the program used to control the vehicle. "QGroundControl provides full flight control and mission planning for any MAVLink enabled drone" [22]. Figure 2.3 displays how an XBox controller was setup, to be used in conjunction with an XBox wireless adapter, to control the vehicle. Four LiPo 14.8 V batteries were used interchangeably throughout the experiment since the vehicle only needs one to run. A Duratrax Onyx 225 battery charger kept the batteries charged and ready to be swapped when necessary. A vacuum pump was used to perform a vacuum test prior to deploying the UUV. Figure 2.4 shows the operation setup for the BlueROV2.

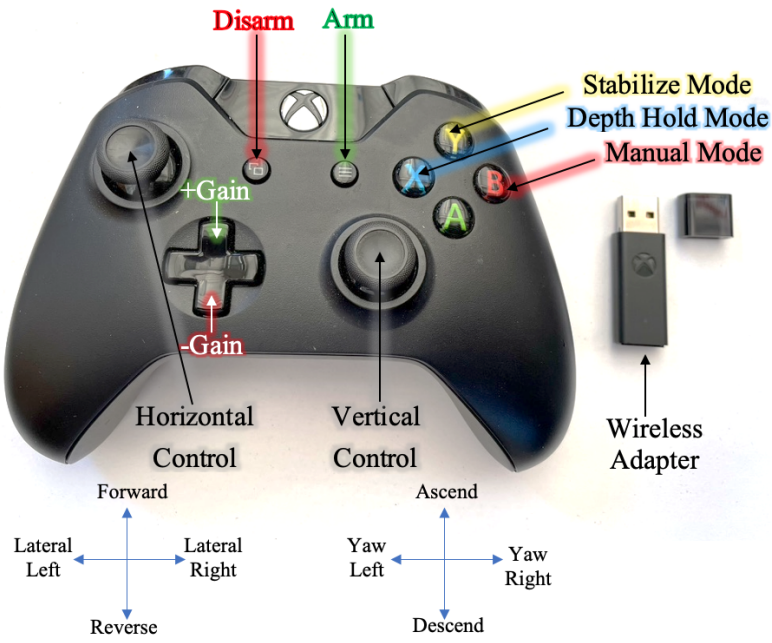

Figure 2.3. XBox Controller and Wireless Adapter. Image shows the XBox controller and the wireless adapter along with the controller functions used during testing.

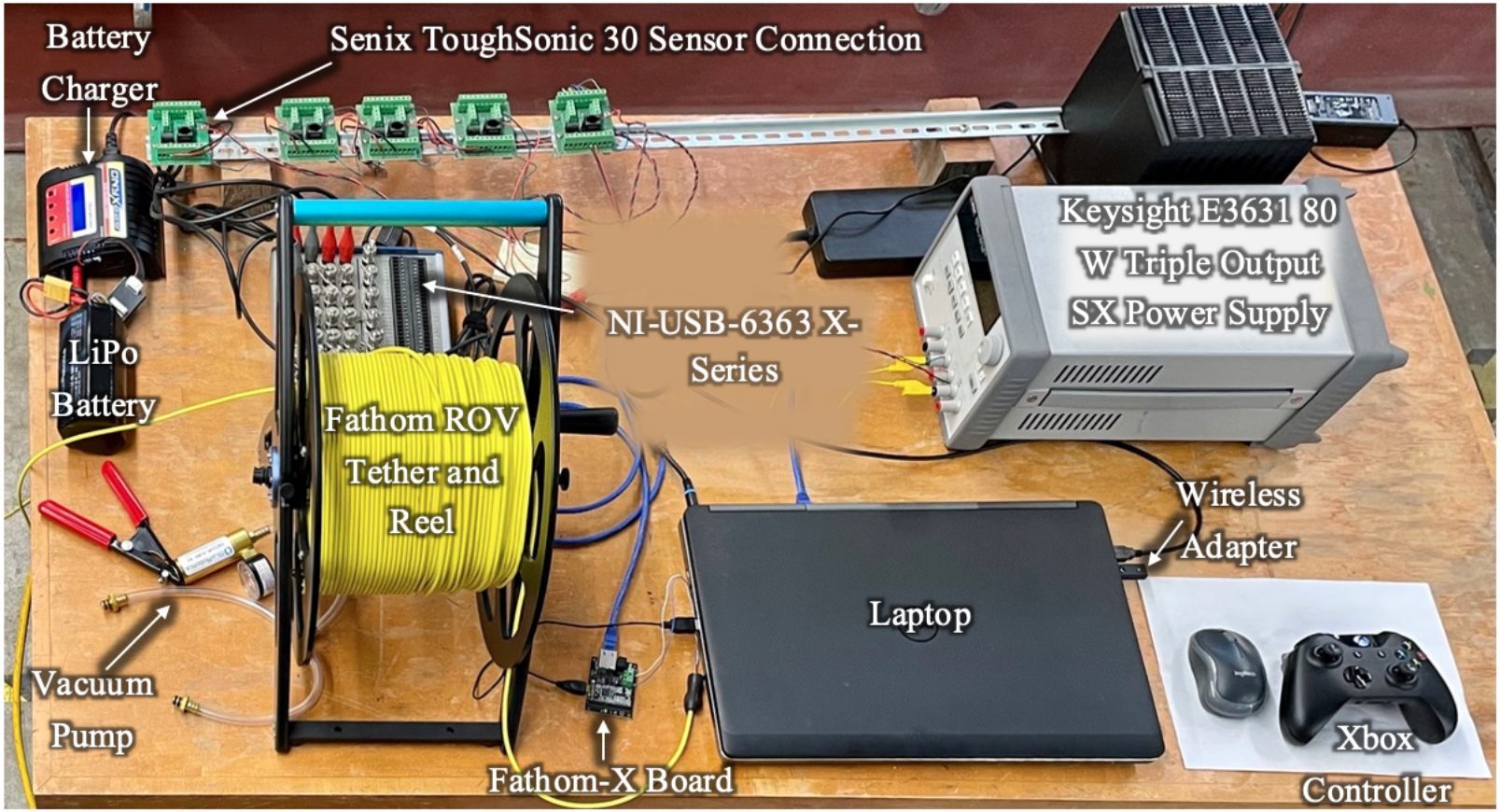

Figure 2.4. BlueROV2 Operation Setup. Photograph showing the BlueROV2 operation equipment and setup used to operate the BlueROV2 and collect carriage position.

The BlueROV2 has three operating modes: Manual Mode, Stabilize Mode, and Depth Hold Mode. In Manual Mode, the vehicle is controlled solely by user input via the XBox controller. In Stabilize Mode, vehicle vertical motion is controlled solely by user input, however, a feedback loop is used to stabilize roll and maintain heading whenever a turn command is not being received. The Depth Hold Mode employs user input to control the vehicle via the remote controller, as well as a feedback loop to maintain depth when no dive/ascend command is present and another to stabilize roll and maintain heading whenever a turn command is not received [23].

2.5 Synthetic Marine Vegetation

The synthetic giant kelp and eelgrass used for this investigation was manufactured by the Bio Models Company. "The Bio Models Company specializes in the production of custom exhibit models" (mostly synthetic plants) "for museum and aquarium displays" [24]. This allowed for a simulation of a littoral environment without the extra work required to maintain live marine vegetation. Plastic that is flexible, durable, and buoyant, but heat sensitive [25] was used to make the synthetic giant kelp and the synthetic eelgrass. Because of their heat sensitivity, they must be kept away from direct sunlight and other heat sources to avoid distortion, damage or melting [25].

2.5.1 Synthetic Giant Kelp

Figure 2.5 shows a single synthetic giant kelp strand. Various numbers of these strands, up to a maximum of 20 strands, were used for the different giant kelp density runs. Each strand is 91.44 cm (36") long and contains ten blades of varying sizes (smaller sizes at the top and largest ones near the bottom), which are attached to a stripe via gas bladders. The strands were attached to the marine vegetation configuration plate using pre-drilled holes and 5.08 cm (2") long, 3/8"-16 nylon threaded anchors at the holdfast.

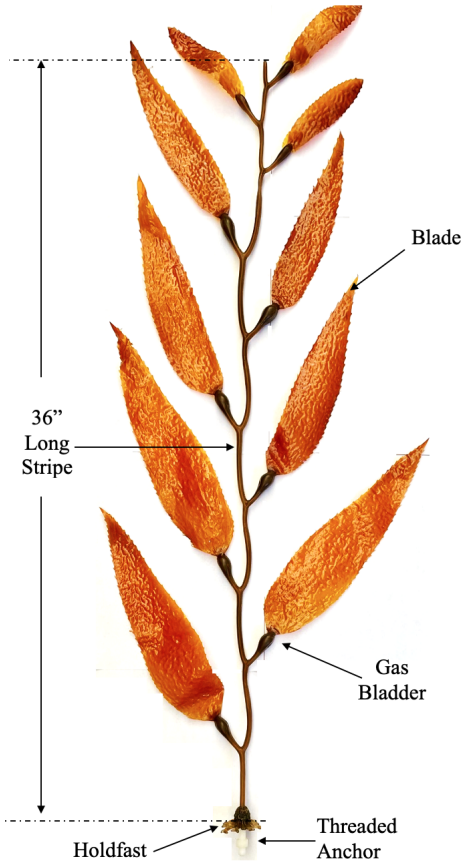

Figure 2.5. Synthetic Giant Kelp. Image of a synthetic giant kelp strand showing the 36 inch long stripe, a holdfast with attached threaded anchor, ten gas bladders, and ten blades.

As part of a previous marine vegetation study [20], [21], a marine vegetation characterization was performed on the synthetic giant kelp, and a single piece of real giant kelp. Table 2.1 shows the results of the physical and material properties tested. The percentage difference shown in the table was calculated using Equation 2.1.

$$\% \text{ Difference} = \frac{\text{Synthetic} - \text{Real}}{\text{Real}} \times 100\% \tag{2.1}$$

Table 2.1. Giant Kelp Characterization. Adapted from: [20], [21].

Material Property	**Real Giant Kelp**	**Synthetic Giant Kelp**	**Percentage Difference (%)**
Stripe Length (cm)	81.28 ± 0.2	90.4875 ± 0.2	11.328
Stripe Diameter (cm)	0.305 ± 0.03	0.65 ± 0.03	113
Blade Length (cm)	41.275 ± 0.2	31.59125 ± 0.2	-23.46
Blade Width (cm)	10.95 ± 0.2	3.19 ± 0.2	-70.87
No. of Blades	18	10	-44.44
Blade Spacing (cm)	4.6 ± 0.2	10.95 ± 0.2	138
Blade Density (blades/cm)	0.2215	0.1105	-50.1
Mass (g)	208.03 ± 0.01	141.11 ± 0.01	-32.17
Volume Displaced (mL)	200 ± 14.3	150 ± 14.3	25
Density (g/mL)	1.04015	0.94073	-9.56
Buoyant Ratio	1.015	0.9415	-7.24

In the previous marine vegetation characterization study, synthetic and actual giant kelp were cantilevered over the edge of a work bench and the resulting vertical displacement at the end of the vegetation was measured. Figure 2.6 shows the deflection for the synthetic and real giant kelp for a range of cantilevered distances from 2.54 to 30.48 cm in 2.54-cm increments (1 to 12 inches in 1-in increments) suspended over the edge of a flat surface [20]. Equation 2.1 was again used to calculate the percentage difference between the synthetic and actual giant kelp. Table 2.2 is a summary of the results.

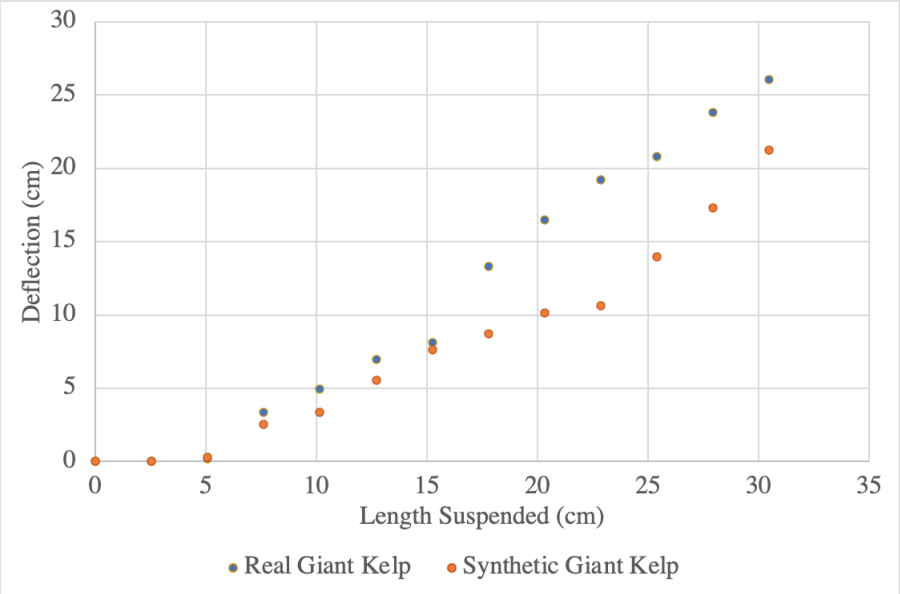

Figure 2.6. Deflection Results for Synthetic and Real Giant Kelp. Adapted from: [20], [21].

Table 2.2. Percentage Difference for Deflection of Synthetic and Real Giant Kelp. Adapted from: [20], [21].

Length Suspended (±0.2 cm)	**Real Giant Kelp Deflection (±0.2 cm)**	**Synthetic Giant Kelp Deflection (±0.2 cm)**	**Percentage Difference (%)**
0	0	0	0
2.54	0	0	0
5.08	0.16	0.32	100
7.62	3.33	2.54	-23.81
10.16	4.92	3.33	-32.26
12.7	6.99	5.56	-20.45
15.24	8.12	7.62	0
17.78	13.34	8.73	-34.52
20.32	16.51	10.16	-38.46
22.86	19.21	10.64	-44.63
25.4	20.80	13.97	-32.82
27.94	23.81	17.30	-27.33
30.48	26.04	21.27	-18.29

2.5.2 Synthetic Eelgrass

Figure 2.7 is an image of a single synthetic eelgrass strand. Different combinations of numbers of these strands, up to a maximum of 29 strands, were used for the different eelgrass density runs. Each strand contained four groups of five 91.44 cm (36") blades, for a total of 20 blades per synthetic eelgrass strand. The width of the blades varied from 0.476 cm (3/16") to 0.635 cm (1/4") and the color was either green (mostly) or light brown. The strands were anchored to the marine vegetation configuration plate via a 5.08 cm (2") long, 1/4"-20 nylon screw.

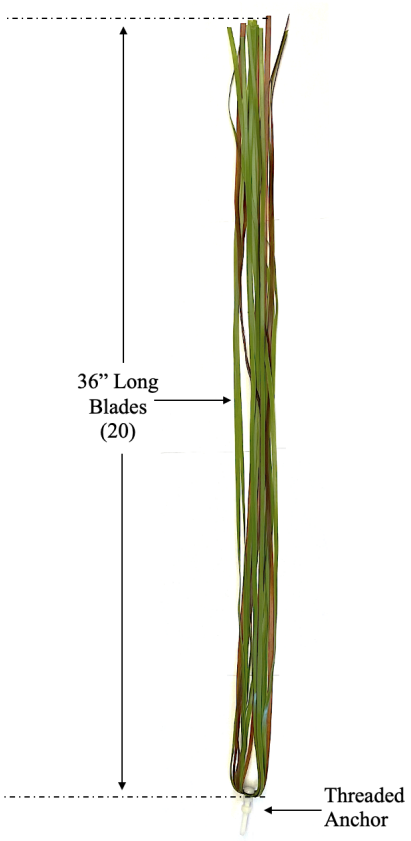

Figure 2.7. Synthetic Eelgrass Strand. Image showing a single synthetic eelgrass strand made up of 20 36-inch long blades and an attached threaded anchor.

Physical and material properties for the synthetic eelgrass were measured previously [20]. Due to the lack of availability of a real eelgrass sample, a comparison was not conducted between the synthetic eelgrass and an actual one. Table 2.3 shows the physical and material properties of the synthetic eelgrass.

Table 2.3. Material Properties for the Synthetic Eelgrass Sample. Adapted from: [20], [21].

Material Property	**Synthetic Eelgrass**
Number of Blades	30
Blade Length	91.44 ± 0.2 cm
Blade Width	0.5556 ± 0.03 cm
Blade Thickness	0.0397 ± 0.03 cm
Mass	37.68 ± 0.01 grams
Volume Displaced	57.2 ± 14.3 mL
Density	0.6587 g/mL
Buoyant Ratio	0.686

Table 2.4 shows the deflection measured for the synthetic eelgrass for a range of cantilevered lengths from 2.54 cm to 15.24 cm (1" to 6") in 2.54 cm (1") increments [20]. Past roughly 15.24 cm, the eelgrass hung vertically down and had no ability to support itself under its own weight.

Table 2.4. Deflection of Synthetic Eelgrass Sample. Adapted from: [20], [21].

Length Suspended (±0.2 cm)	**Deflection (±0.2 cm)**
2.54	No Deflection
5.08	0.635
7.62	3.81
10.16	7.62
12.7	10.795
15.24	15.24

2.6 Marine Vegetation Configuration Plate

A 0.914 m by 0.61 m (3' by 2') Plexiglas plate with pre-drilled holes was used as a marine vegetation configuration plate, shown in Figure 2.8. The synthetic giant kelp or eelgrass strands were attached to this plate using their respective anchors. The density configuration was easily changed from single, low, medium, or high using this plate. Up to 35 (five columns with seven rows) synthetic giant kelp could be attached by utilizing the 3/8" clearance holes, and up to 30 (6 columns with five rows) synthetic eelgrass could be attached utilizing the 1/4" clearance holes. Four larger corner holes were used to attach ropes to use to lower and lift the plate in and out of the tank. A 9.07 kg (20-lb) weight, also attached to some rope, was used to hold the plate in place, shown in Figure 2.9.

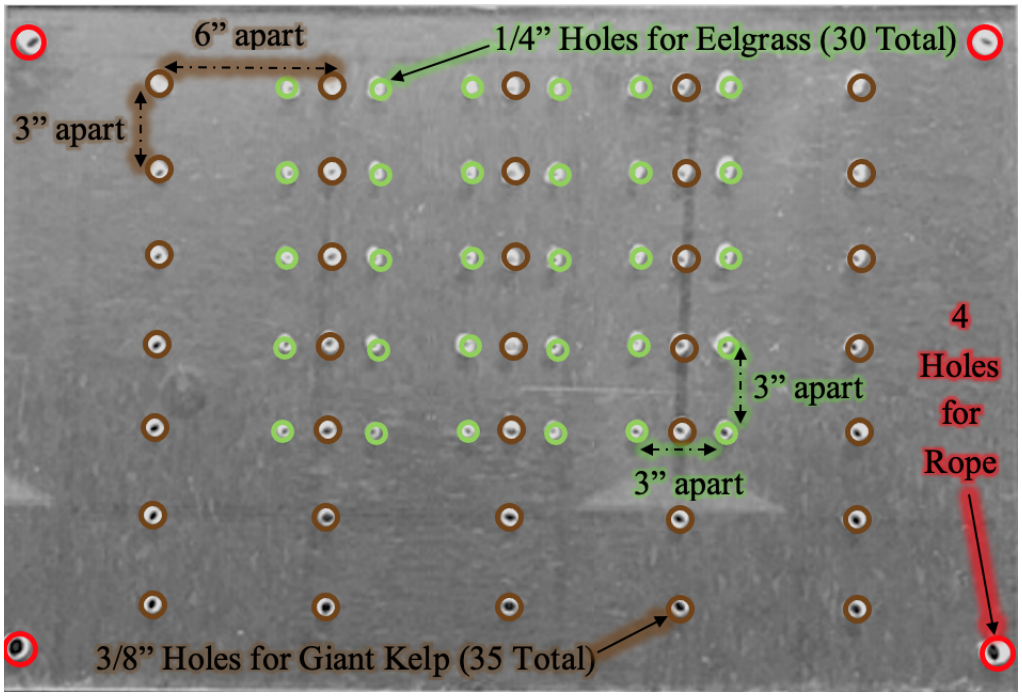

Figure 2.8. Vegetation Configuration Plate. The vegetation configuration plate is made of plexiglass with pre-drilled holes to change vegetation type and density. Adapted from: [20].

Figure 2.9. Image of 9.07 kg (20-lb) Weight. This weight was used to keep vegetation configuration plate from moving.

2.7 Chapter Summary

The experiments were conducted in the hydrodynamics lab in Halligan Hall at NPS. The BlueROV2 UUV was attached to the towing tank carriage using a vertical sting, a 3D printed adapter, a U-channel, and two machined L-brackets. The UUV communicated to a laptop using QGroundControl software, a 100-meter Fathom tether cable on a Fathom spool, a Fathom-X board, and an Ethernet cable. An Xbox controller with a wireless adapter was configured to be used with the QGroundControl software to control the UUV. Up to 20 strands of synthetic giant kelp and 29 strands of synthetic eelgrass were anchored to a Plexiglas plate used as a marine vegetation configuration plate, to vary the vegetation type and density during testing. Rope was used to aid with the insertion and removal of the Plexiglas plate and a 20-pound weight from the tank.

CHAPTER 3:
Calibration and Experimental Procedures

Chapter 3 discusses the procedures used for this thesis. Calibration runs were performed to estimate the vehicle's speed while attached to the carriage for a given gain setting. Three different gain settings, corresponding to three different speeds, were chosen to carry out the experiment. The experimental runs were then conducted with these speeds and different types and densities of synthetic marine vegetation for each speed. Both the calibration runs and the experimental runs were done using the same equipment and procedures that previous marine vegetation entanglement studies at NPS [20], [21] used with the exception of the UUV specific related equipment and procedures.

3.1 BlueROV2 Pre-Dive Checks

Before lowering the vehicle into the water, the pre-dive checks listed in the BlueRobotics website were conducted. The battery enclosure was opened and a charged LiPo battery was connected, then the battery enclosure was closed. The UUV was connected to the laptop using the Fathom tether cable, the Fathom-X board, an Ethernet cable, and a USB cable. The QGroundControl program was opened and the battery level checked to ensure sufficient charge (14-16 V). The battery was never used below 12.8 V per Blue Robotics guidance [23]. Then a check to confirm that there are no error or warning banners showing in the program and that the lights and camera are operating properly was conducted (proper camera operation was not needed for this experiment). Integrity of the vehicle was confirmed visually and physically, checking that all the enclosures are properly closed, plugs were installed, and that there were no loose, cracked or sliced parts [23]. Using the software, and the controller, the vehicle was tested for proper operation by arming it and spinning the forward/reverse and ascend/descend thrusters in manual mode, then disarming.

A vacuum test was required prior to deploying the vehicle for the first time or whenever anything that might compromise the seal has happened or was suspected of happening [23]. Out of precaution, the vacuum test was done prior to deploying the vehicle anytime the battery enclosure was opened. The vacuum test consists of removing the vent plugs off the battery and electronic enclosures, connecting a vacuum pump on those ports, pumping until the pump's gauge reads 33,863.9 Pa (10 in Hg), and then waiting 15 minutes to see if a leak exists. If the pump's gauge reads between 30,477.5 Pa (9 in Hg) and 33,863.9 Pa (10 in Hg), then the test was satisfactory [23]. If the vehicle did not hold vacuum, then the enclosures and O-rings are visually checked, tightened or replaced (as necessary) and the test was repeated.

3.2 Vehicle Speed Calibration

Prior to the calibration runs, the tank was filled to a water depth of 91.44 cm (36") and the vehicle's pre-dive checks were conducted. The handle and sting were attached to the BlueROV2, and then mounted to the tank's carriage. The Plexiglas plate was mounted on the tank's carriage, and its position was measured using the Senix ToughSonic 30 Ultrasonic Position Sensor Model TSPC-15S, whose power and laptop connection is described in Section 2.1. A MATLAB script, using the data acquisition toolbox, collected the digitized voltages from the NI DAQ board and stored them on a laptop computer. The program was set to record 30 seconds of data.

Using the XBox controller and the QGroundControl program, the gain setting for the vehicle was adjusted from 20% to 100%, at 10% increments, and the vehicle was controlled in Manual Mode to move from the one end of the tank to the other end. This was done for 30 seconds or until the vehicle reached the end of the tank, whichever happened first. Once the vehicle reached the end of the tank (or was moved by-hand with the carriage to the end of the tank) the vehicle was operated in the opposite direction (for the initial calibration runs) or was moved by hand to the same starting point (follow-on calibration runs). Because the joystick used for horizontal speed control had a continuous input range, depending on how far the throttle was pushed toward the desired direction, every run was performed by using full throttle (joystick pushed all the way of the desired direction). This made the gain setting the deciding factor on vehicle speed and made the runs fairly repeatable, assuming no significant change in battery voltage.

Initially, three runs were performed for all of the vehicle gain settings in both forward and astern operations, with the exception of the 40% and 50% gain runs, which had five and eight runs per direction. These addition runs were due to performing additional 40% and 50% gain runs in between the sets of other gain runs. Follow-on calibration runs were only done on chosen gain settings for low, medium and high speed, described in the next section. For these runs the vehicle was operated only in the forward direction and three runs were done per setting.

3.2.1 Calibration Analysis Method

A MATLAB file, named DataCleaner, was used to "clean" the data by removing any data outliers and converting the collected voltages to physical units. The voltage output was converted to a position in physical units using a sensor gain of 76.2 centimeters per volt (30 inches per volt). While running the DataCleaner, a plot of position versus time was produced and four different points were selected: the point where the vehicle started moving, where steady-state was first reached, where steady-state ended, and where the run was stopped. These four points were recorded and used in another MATLAB file that estimated the vehicle's speed. Once the program completed it wrote a .dat ASCII file that

was subsequently used to estimate the velocity.

A final MATLAB file was used to estimate the actual velocity using the output from the DataCleaner and two different approaches. The first approach was a simple linear polynomial fit method, and the second was using a physics-based model. For the linear polynomial fit, the program used the selected points two and three, leaving only the steady state portion for the linear regression analysis and removing the acceleration and deceleration portions. The slope of the linear regression was used to estimate the vehicle's steady state speed.

For the second approach, a physics-based model was used. This model was based on the application of Newton's second law to the UUV. Equations 3.1 to 3.3 cover the mathematical derivation for this method's estimates. The net force on the UUV will produce an acceleration given by

$$\sum F_i = T - D = ma \tag{3.1}$$

where F_i is an individual force acting on the vehicle, T is the thrust force, D is the drag force, m is the vehicle's mass and a its acceleration [20]. With the assumption that the thrust was only a function of the propeller speed, which was fixed during a given run, and does not depend on the actual relative velocity of the flow into the propeller, which changes as the vehicle accelerates. It was also assumed that the drag coefficient was constant for a given run. The drag coefficient is a function of Reynolds number but the Reynolds number range covered for a given run was small enough to allow this assumption. The validity of these assumptions was verified by the high level of accuracy that the derived expression for position as a function of time was able to model the measured position data time history. Apply our assumptions, Equation 3.1 becomes

$$\frac{dv}{dt} = \frac{T}{m} - \frac{\frac{1}{2}\rho S_a C_d}{m} v^2 \tag{3.2}$$

where dv/dt is the derivative of velocity with respect to time, ρ is the water density, S_a is the vehicle's cross-sectional area, C_d is the drag coefficient, and v is the vehicle speed [20]. Equation 3.2 can be integrated to find an expression for the vehicle's velocity as a function of time, given by Equation 3.3, using the initial condition $v(0) = 0$ [20], and the unknown constant values represented by coefficients A and B, shown in Equations 3.4 and 3.5, respectively.

$$v(t) = \sqrt{\frac{A}{B}} \tanh(\sqrt{AB}t) \tag{3.3}$$

$$A = \frac{T}{m} \tag{3.4}$$

$$B = \frac{\frac{1}{2}\rho S_a C_d}{m} \tag{3.5}$$

3.2.2 Calibration Example

A speed calibration run using a 40% gain setting is provided in this section as a sample of the data analysis process. Voltage and time data was collected as discussed in Section 3.2 and exported as a .csv file [20]. A MATLAB script called this file to solve and plot position versus time and speed versus time [20], the results are shown on Figure 3.1. Figure 3.1(a) shows the measured position of the vehicle as a function of time (blue line) with a linear regression for the steady state speed (green line) and a curve fit from the physics-based model (red line) [20]. Figure 3.13.1b shows the vehicle speed vs time as a blue line and the vehicle steady state speed vs time with a red line [20], [21]. Equation 3.3 was used to determine the vehicle's speed as a function of time and the linear regression was used to estimate the vehicle's steady state speed.

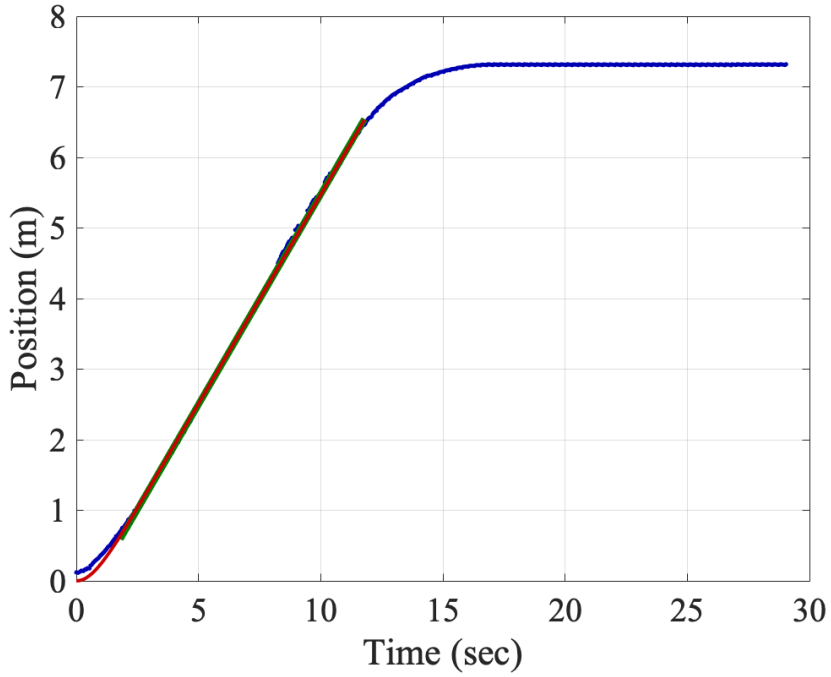

(a) BlueROV2 position as a function of time.

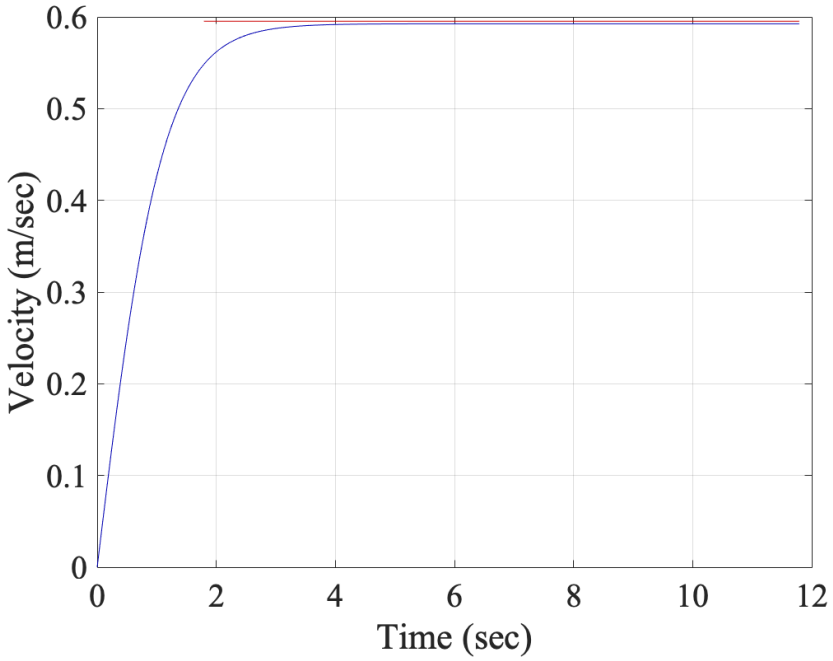

(b) BlueROV2 speed as a function of time.

Figure 3.1. Speed Calibration Results for 40% Gain.

3.2.3 Calibration Results

Table 3.1 shows the results for the initial calibration runs. Because of the vehicle's symmetry, the experimental runs were only conducted using with forward vehicle operation, with the exception of the unrestricted movement runs. Only the forward operation estimates are shown. The estimates were converted from feet-per-second to meters-per-second, and an average value was calculated for each setting.

Table 3.1. BlueROV2 Initial Calibration Table.

Gain (%)	**Average Battery (V)**	**Velocity (ft/s)**	**Velocity (m/s)**
20	15.783	0.89 ±0.16	0.27 ±0.05
30	15.683	1.49 ±0.05	0.45 ±0.02
40	15.450	1.96 ±0.08	0.60 ±0.025
50	14.625	2.30 ±0.16	0.70 ±0.05
60	15.067	2.67 ±0.26	0.82 ±0.08
70	14.850	2.97 ±0.80	0.91 ±0.24
80	14.450	3.18 ±0.21	0.97 ±0.06
90	14.000	3.30 ±0.44	1.01 ±13
100	13.400	3.19 ±0.27	0.97 ±0.08

After performing the initial calibration runs, and estimating the velocities for each gain setting, three different gain settings were chosen for the restricted movement runs. The basis for the chosen gain settings was to get three velocities as closest as possible to the ones used in the previous work for low, medium and high velocities. The gain settings chosen were 20%, 40% and 80% for estimated velocities of 0.271 m/s, 0.598 m/s and 0.97 m/s, respectively. However, because the battery voltage has an effect on the propeller's angular velocity for a given commanded velocity, and therefore the UUV's achieved velocity, additional calibration runs were performed for these three gain settings, all at battery voltages closer to the UUV's battery voltage during the experimental runs. Table 3.2 shows the results for the follow-on calibration runs performed for the chosen vehicle gain settings.

Table 3.2. BlueROV2 Follow-On Calibration Table.

Gain (%)	Average Battery (V)	Velocity (ft/s)	Velocity (m/s)
20	15.633	0.74 ±0.003	0.23 ±0.001
40	15.657	2.02 ±0.01	0.62 ±0.003
80	15.730	3.37 ±0.04	1.03 ±0.012

When comparing the velocities obtained in the initial calibration table with the follow-on calibration table for the chosen experimental gain values, it is apparent that higher battery voltage leads to slightly higher velocities; however, this was shown to be of very little effect. In order to minimize this, the experimental runs were conducted with vehicle battery levels between 15 V and 16.2 V.

3.3 Experimental Procedures

The experimental runs consisted of changing marine vegetation type (two types: giant kelp and eelgrass), marine vegetation density (four configurations: high density, medium density, low density and single strand) and UUV speed, and noting any interactions between the vehicle and the marine vegetation. The number of runs per setting and vehicle direction varied across the runs. On some occasions the number of runs performed was dependent on previously seen interactions and the current condition of the available synthetic marine vegetation. The iteration number, vegetation type and density, vehicle gain and battery charge as well as the resulting interactions were annotated for each run. The vehicle speed and movement was controlled using the horizontal control joystick and gain settings as described in the first paragraph of Section 3.2, using full throttle of the joystick to make the runs repeatable. The Design of Experiment (DOE) is shown on the applicable results table in Chapter 4.

3.3.1 Experimental Setup

Prior to the calibration runs the tank was filled to the 91.44 cm (36”) mark and the vehicle’s pre-dive checks from Section 3.1 were conducted. The Vegetation Configuration Plate was set-up with the desired vegetation type and density, as seen in Figure 3.2 and Figure 3.3, and lowered into the middle section of the tank using ropes. A 9.07 kg (20 lb) weight was used to keep the vegetation configuration plate from moving, as mentioned in Section 2.6.

Figure 3.2 shows the high density, medium density, low density and single strand giant

kelp configurations on the marine vegetation configuration plate using brown circles. The distance between giant kelp strands was changed by 6” for each of the density configurations (with the exception of the single giant kelp configuration).

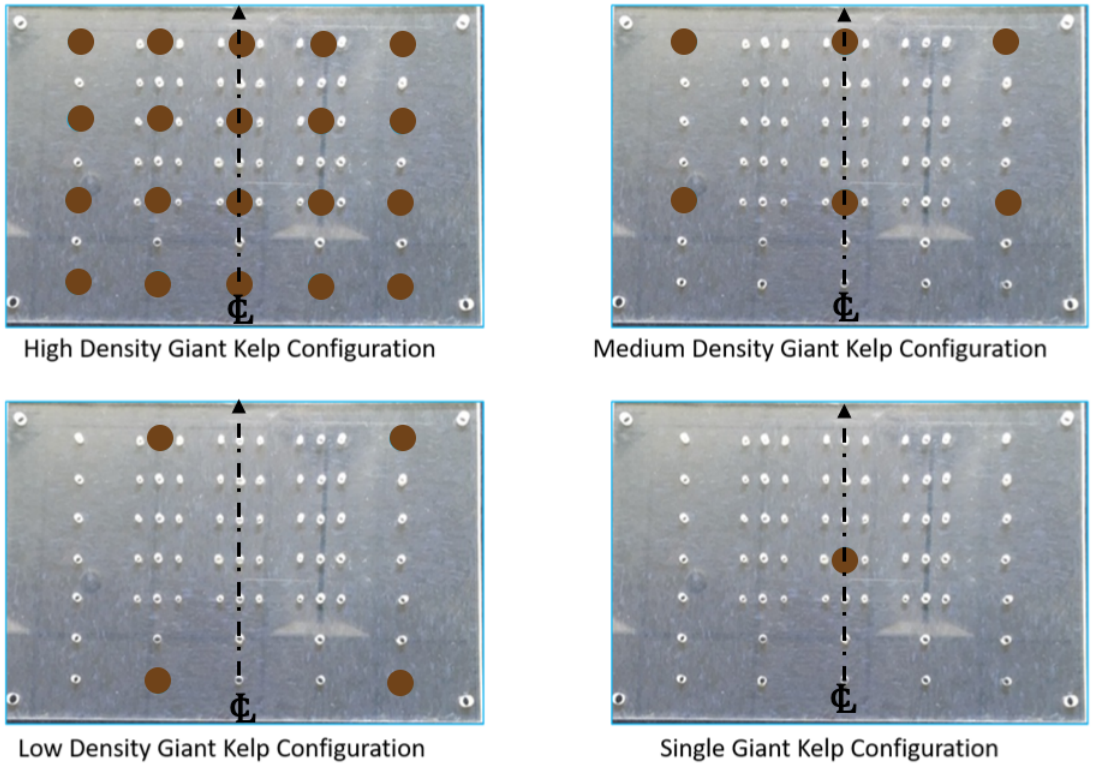

Figure 3.2. Giant Kelp Configurations. Marine vegetation configuration plate showing the different giant kelp density configurations used. Adapted from: [20], [21].

Figure 3.3 shows the high density, medium density, low density and single eelgrass configurations on the marine vegetation configuration plate using green circles. A white circle is used in place of a green one on the top right corner of the high density eelgrass configuration plate, since only 29 synthetic eelgrass strands were available due to some strands being damaged from earlier testing. The distance between eelgrass strands was changed by 7.62 cm (3”) for each of the density configurations (with the exception of the single eelgrass configuration).

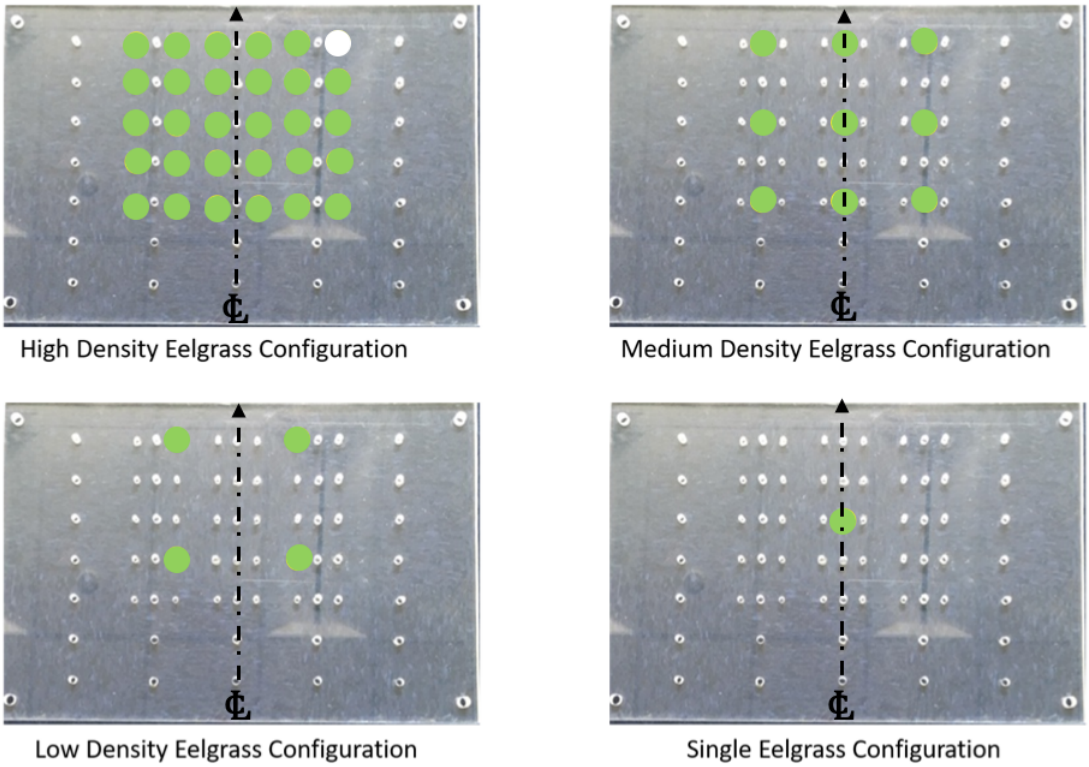

Figure 3.3. Eelgrass Configurations. Marine vegetation configuration plate showing the different eelgrass density configurations used. Adapted from: [20].

Table 3.3 shows the different synthetic marine vegetation densities for the experimental configurations. Note that the areas used in the density calculations are different for the giant kelp and the eelgrass. The area used for the giant kelp density calculation is based on the plate area where the giant kelp can be anchored to, which is 0.2787 m^2 (3 ft^2) and the area used for the eelgrass density calculation is based on the plate area where the eelgrass can be anchored to, which is 0.1161 m^2 (1.25 ft^2).

Table 3.3. Synthetic Marine Vegetation Densities for Experimental Configurations. Adapted from: [20], [21].

Configuration	Plant Type	No. of Plants	Density (plants/ft^2)	Density (plants/m^2)	Spacing (in)
Single	Giant Kelp	1	0.33	3.59	CL*
Low Density	Giant Kelp	4	1.33	14.35	18
Medium Density	Giant Kelp	6	2	21.53	12
High Density	Giant Kelp	20	6.67	71.76	6
Single	Eelgrass	1	0.8	8.61	CL*
Low Density	Eelgrass	4	3.2	34.44	9
Medium Density	Eelgrass	9	7.2	77.5	6
High Density	Eelgrass	29	23.2	250	3

*CL indicates centerline.

3.3.2 Unrestricted Movement Runs

Runs were made prior to choosing the DOE, without the use of the testing fixture, to observe the unbiased operation of the BlueROV2 with different giant kelp densities and at different speeds as well as different movement direction (forward and astern movement). For these runs the vehicle was operated in Depth Hold Mode. These runs were first performed using the high density giant kelp configuration and changing the vehicle's gain (for speed) from 10% to 100%, in 10% increments. Three runs were performed for forward movement and three for astern movement. This was repeated for the medium density giant kelp, but only for gain values of 30%, 50%, 70% and 90%. For the low density and single giant kelp densities, only the gain values 30%, 50% and 70% were tested. Only the single density and the 50% gain runs were performed for the eelgrass vegetation due to severe entanglement and damage to the synthetic eelgrass strands.

3.3.3 Restricted Movement Runs

When operating in the unrestricted configuration, the experimental runs were not repeatable since the vehicle was free to change orientations. For these sets of experimental runs, the BlueROV2 was attached to the tank's carriage via the sting and adapter using holes nine and 14 on the sting, as mentioned in Section 2.2. The experiment was started using the

single giant kelp vegetation configuration. The BlueROV2 was connected to the laptop as described in Section 2.4 and the program QGroundControl and Xbox controller were used to control it. Using the Xbox controller, the gain was adjusted to 80%, the vehicle was armed and verified in Manual Mode. Then using the horizontal control joystick (at full throttle) the vehicle was controlled to move from one end of the tank to the other.

The experiment was repeated with the same vegetation configuration and vehicle gain setting up to ten times, depending on the interactions noted and their variation. Once a satisfactory number of runs had been conducted, the vehicle gain setting was adjusted to the next gain setting (40%, and then 20%) without changing the vegetation configuration, and the experiment was repeated. If significant damage was observed on one or more of the synthetic marine vegetation plants, the configuration plate was raised using the ropes and the affected synthetic strand were swapped as necessary. Once all three vehicle speeds have been tested with a vegetation configuration, the vegetation density was changed (from single to low density, medium density and high density) and the experiment was repeated. The position of the carriage plate was measured using the Senix probe in the same manner as the calibration runs for some additional high density giant kelp runs at 40% and 80% gain values. This allowed the vehicle speed changes through the vegetation to be estimated. Once all vegetation densities had been tested for giant kelp, the experiment was repeated with eelgrass. The order of the vegetation types or densities was not significant; however the one mentioned in this section was chosen based on the lowest expected interaction first.

THIS PAGE INTENTIONALLY LEFT BLANK

CHAPTER 4:
Results and Analysis

This chapter presents the results of this investigation. The interactions that occurred were dependent on the vegetation type. Based on previous work, the expected interactions were: no entanglement, occlusion, and entanglement. Any interaction that was observed would occur with the vehicle's propeller [20], [21]. The BlueROV2's boxy-design, as well as the gaps between its multiple sub-components, caused entanglement of the synthetic giant kelp strands with the vehicle's body itself. The giant kelp, when in a high enough density, also caused blockage, preventing the vehicle from advancing any further into the vegetation. The term "blockage" is used when there are no indications of entanglement with the vehicle's body or propellers, but the vehicle is unable to move any further through the vegetation. On occasions there was complete blockage, meaning the vehicle was unable to enter the vegetation. The vehicle's interaction with the synthetic eelgrass were more attuned with the expected results, in that entanglement only occurred within with the vehicle's propellers.

4.1 Synthetic Giant Kelp Interactions

There was a wide range of interactions between the BlueROV2 and the synthetic giant kelp. Runs were made with and without the test fixture to see how much the test fixture affected the observed outcome. The unrestricted runs were performed first, starting with the high density giant kelp configuration. Based on those results, the next speed (gain) values were selected for the medium density runs. The same was done to select the speeds (gain) for the low and single density runs. The runs performed with the test fixture were only performed at three speeds: low speed (20% gain), medium speed (40% gain), and high speed (80% gain). These were the gain settings that produced the vehicle speeds closest to the ones from the previous work.

4.1.1 Unrestricted Movement Runs

Figure 4.1 shows the results for the unrestricted experimental runs without the testing fixture, using the depth hold operating mode. For this run type there were four different resulting interactions. The interaction labeled with the number zero was no entanglement. In this case the vehicle was able to go through the giant kelp without slowing down or experiencing any blockage or entanglement. The interaction labeled with the number one was used when the UUV slowed down while running over the giant kelp vegetation, but was not entangled or blocked. Interactions labeled with the numbers two and three were both undesired outcomes, since they precluded the vehicle from going through the vegetation. If the vehicle was able

to enter the vegetation, and then got entangled and stuck, the outcome was labeled with the number two. For this interaction, the vehicle would start to run over the vegetation, pushing it downwards and going over it. This caused a depth change for the vehicle, actuating the vertical propellers, which made the probability of propeller entanglement higher (due to a higher number of propellers operating). In the cases where the vehicle entangled, its ability to maintain depth was hindered and the vehicle sank to the floor of the tank, due to its slight negative buoyancy. If the vehicle was not able to go through the vegetation because it was blocked by it, then the outcome was labeled with the number three.

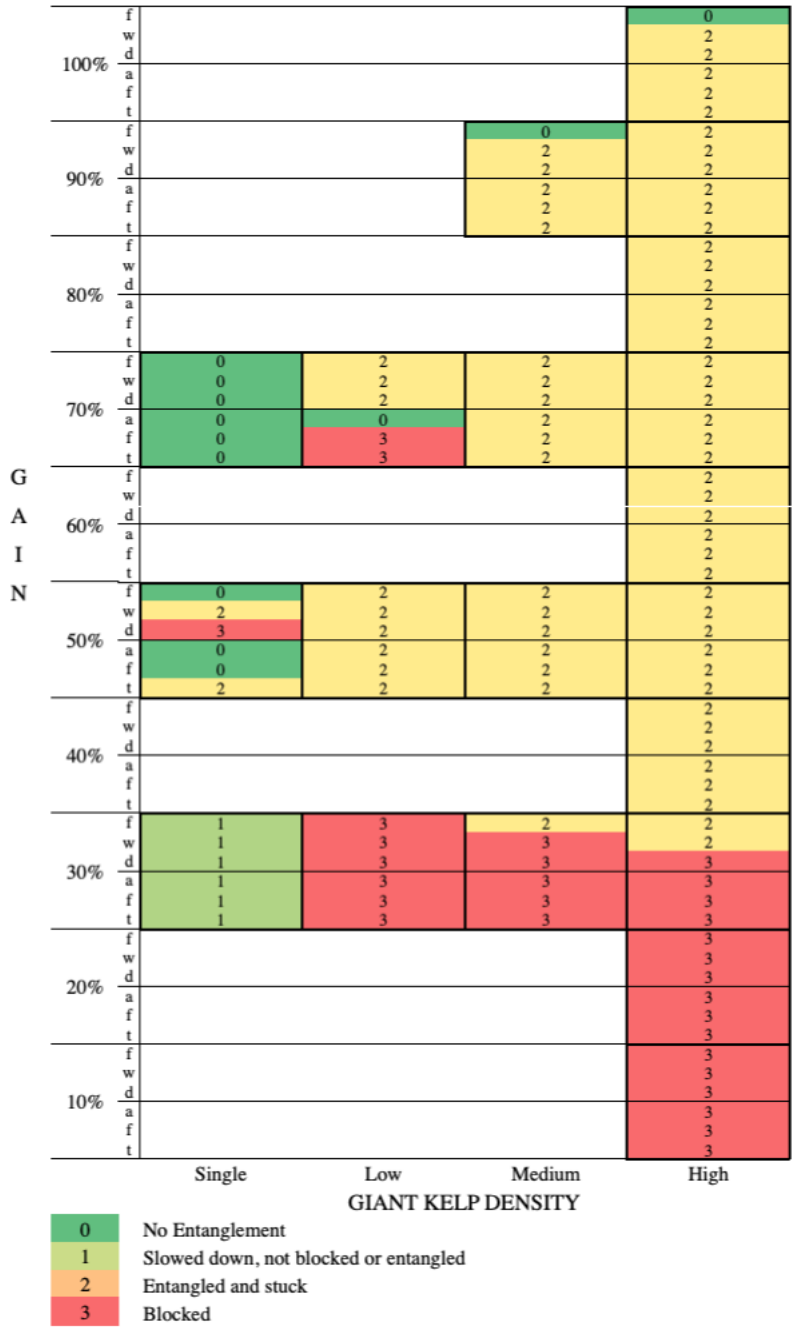

Figure 4.1. Results for Unrestricted Movement Runs with Giant Kelp. Vegetation interaction results for unrestricted runs with giant kelp sorted by vegetation density and vehicle speed.

Single Giant Kelp

All of the runs conducted at 70% gain, on both forward and astern operation, resulted in no entanglement. For the runs at 30% gain, the vehicle slowed down, but was not entangled or blocked. This was the case for both forward and astern operations. For the 50% gain runs the results were not as consistent. The forward operation runs at this speed gave different results for each of the three runs. One time there was no entanglement, one time it was entangled and stuck, and the other time the vehicle was blocked. Astern operations at this speed resulted in no entanglement for two of the three runs and that third run resulted in an entanglement.

Low-Density Giant Kelp

There were consistent results for the BlueROV2 speeds in the 30% and 50% gain settings, but not for the 70% gain setting. For the runs done using the 30% gain setting, the vehicle was blocked by the synthetic giant kelp for all three forward and astern runs, and for the 50% gain setting, the vehicle got entangled and stuck for all the runs. For the runs with speed corresponding to a 70% gain setting, all three of the forward runs resulted in vehicle entanglement, while the astern operations had differing results. For one of the astern runs, the vehicle was able to go through the vegetation without any entanglement. But for the other two occasions, it was blocked and unable to enter the vegetation.

Medium-Density Giant Kelp

The BlueROV2 was able to go through the medium density giant kelp vegetation without entanglement in one of the three forward runs at 90% gain. The other two forward runs and all three of the astern runs at that speed resulted in vehicle entanglement. All of the runs for both forward and astern operation in the 50% and 70% gain also resulted in vehicle entanglement. At the 30% gain setting the vehicle was blocked from entering the medium density giant kelp vegetation all the time during astern operations and two out of three times during forward operation. One of the three forward operation runs at the 30% gain setting resulted on vehicle entanglement.

High-Density Giant Kelp

For the high density giant kelp runs, vehicle entanglement was the most common result observed. As seen in Figure 4.1, the entirety of the results for the runs made between the 40% and 90% gain settings (in 10% gain increments) were of the vehicle getting entangled and stuck. All of the runs made at gain settings 20% and 10% resulted in the vehicle being blocked from entering the vegetation. The only runs that did not show consistent results were those with the 100% and 30% gain settings. In one of the three forward operating runs at 100% gain, the vehicle made it through the vegetation without getting blocked or entangled. In the other two it got entangled and stuck. Two of the three forward operating

runs at the 30% gain setting also resulted in vehicle entanglement. On the other occasion, the vehicle was blocked from entering the high density giant kelp vegetation. All of the runs for the astern operation at 30% gain setting also resulted in the vehicle being blocked.

4.1.2 Restricted Movement Runs

There were nine different interactions observed between the UUV and the synthetic giant kelp for the restricted movement experimental runs. The lowest interaction (labeled as zero) was no adverse interaction, such as entanglement, which was the equivalent of saying no interaction. There was also not even a noticeable change in vehicle speed. The next interaction, labeled as one, was no entanglement but the vehicle slowed down. Due to the vehicle's shape and size, and the rigidity of the synthetic giant kelp strands, there was a significant reduction on vehicle speed as it ran over the vegetation. The term "ran over" is used because instead of pushing the giant kelp to the sides, the giant kelp was pushed forward and downward and the vehicle then passed over it. The interaction labeled with the number two corresponds to the vehicle slowing down with an entangled propeller. For this kind of interaction, one or more giant kelp blades reached at least one of the propellers, entangling and slowing down the UUV. A similar interaction was observed and labeled with the number three. The only difference between interaction two and interaction three was that the propeller was spinning at a fast enough speed that any giant kelp blade entangled was ripped from the stripe. The interaction labeled with the number four was synthetic giant kelp entanglement with the vehicle's body, such that the vehicle kept moving, dragging the plate. The interaction labeled with a number five was similar to this last one, but in this case the vehicle was only able to drag the plate for a very short period of time (one to two seconds) before coming to an all stop. Interaction labeled with the number six consisted of the synthetic giant kelp entangling with the vehicle's body in such a way that it completely stopped the vehicle. Whenever the vehicle's body got entangled with the giant kelp, it was due to the stripe, the gas bladder, or the connection between the two getting trapped within the vehicle's frame. The last two interactions, labeled with the numbers seven and eight, consisted of the synthetic giant kelp blocking the vehicle, not allowing it to enter, and blocking the vehicle but with at least one giant kelp blade reaching one of the vehicle's propellers and wrapping around it.

The various interactions mentioned above caused different types of damage to the synthetic giant kelp. Figure 4.2 shows examples of damaged synthetic giant kelp. Figure 4.2(a) and Figure 4.2(b) show two of the synthetic giant kelp strands after the experimental runs were conducted. Common damage seen throughout were missing blades, damaged blades, and elongated stripes. It was observed that if the giant kelp blades reached a propeller and the vehicle was going at a fast enough speed (mostly at 80% gain, but occasionally at 40% gain), the blade would be ripped from their connection point to the gas bladders. The damaged and missing blades were the result of entanglement with the vehicle's propellers, and the

elongated stripes were the result of entanglement with the vehicle's body. The elongated stripe damage was worse when the synthetic giant kelp strands, along with the vegetation configuration plate, were dragged by the vehicle through the tank. For this reason the vehicle was not allowed to drag the plate for longer than a couple seconds. If the vehicle came to an all stop by itself (even with the signal to keep moving forward), the result was labeled as a BE/D/K (5), else the signal to move forward was removed and the result was labeled as a BE/D (4). Throughout the experimental runs, 16 synthetic giant kelp blades were ripped from the blade-gas bladder connection, seen in Figure 4.2(c): four from the smallest size and highest location, three from the second smallest size and second highest location, six from the second largest and second lowest location and three from the largest and lowest location. There were also five blade segments that were ripped due to repeated propeller damage to the same area. This type of damage can also be seen in Figure 4.2(a) and Figure 4.2(b).

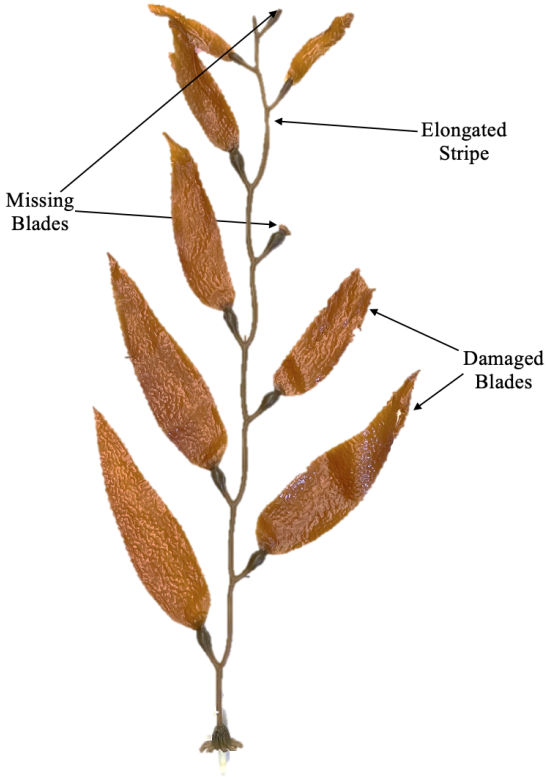

(a) Example of Damaged Giant Kelp Strand.

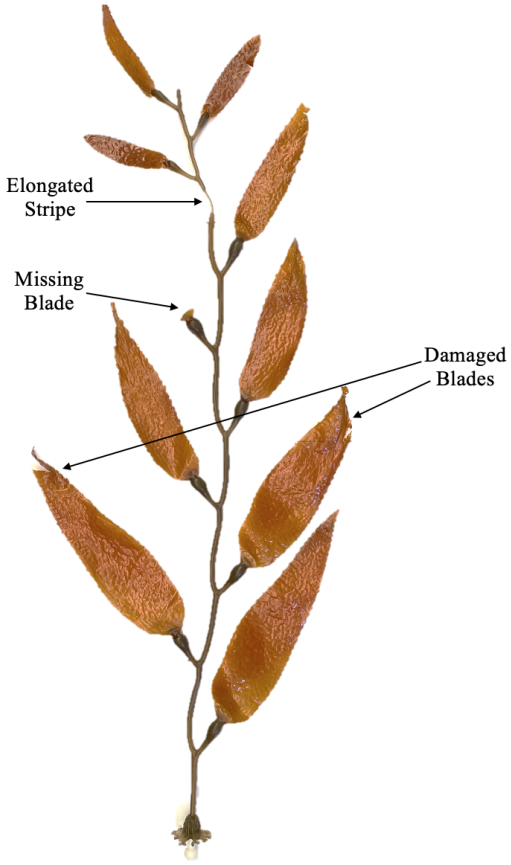

(b) Example of Damaged Giant Kelp Strand.

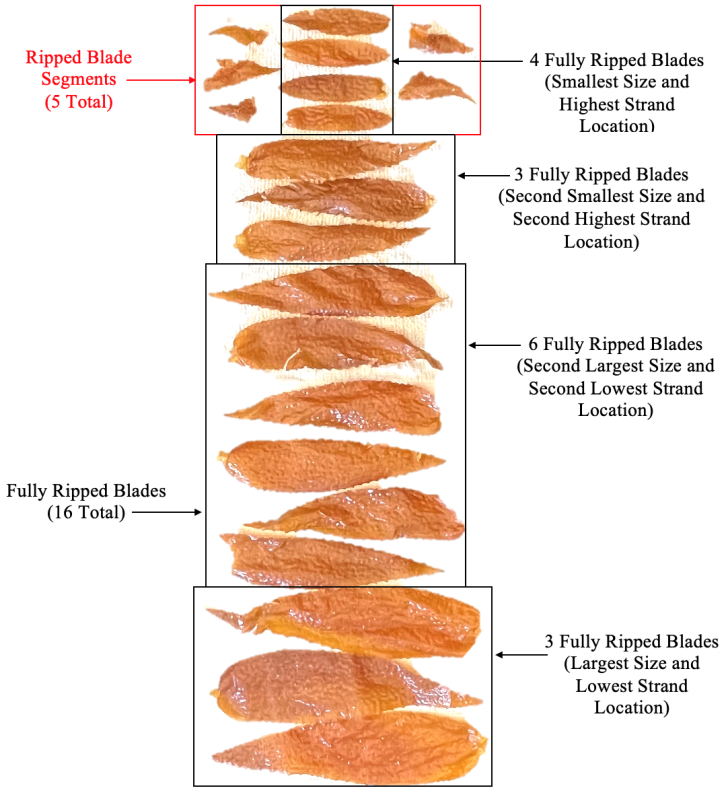

(c) Severed Giant Kelp Blades.

Figure 4.2. Examples of Damaged Giant Kelp.

The results of the restricted movement runs described in Section 3.3.3 can be seen in Figure 4.3. Within a given density and speed combination, the results were sorted based on the level of interaction prior to plotting. The region that showed the best prognosis, or lower levels of interactions, was the highest speed (80% gain) and lowest density (single giant kelp), as expected. The region that showed the worst prognosis was the lowest speed (20% gain) and highest vegetation density (high giant kelp density). It was expected that this region would have the most negative interactions. However, the blockage was not expected, since it was not a resulting interaction on the previous work.

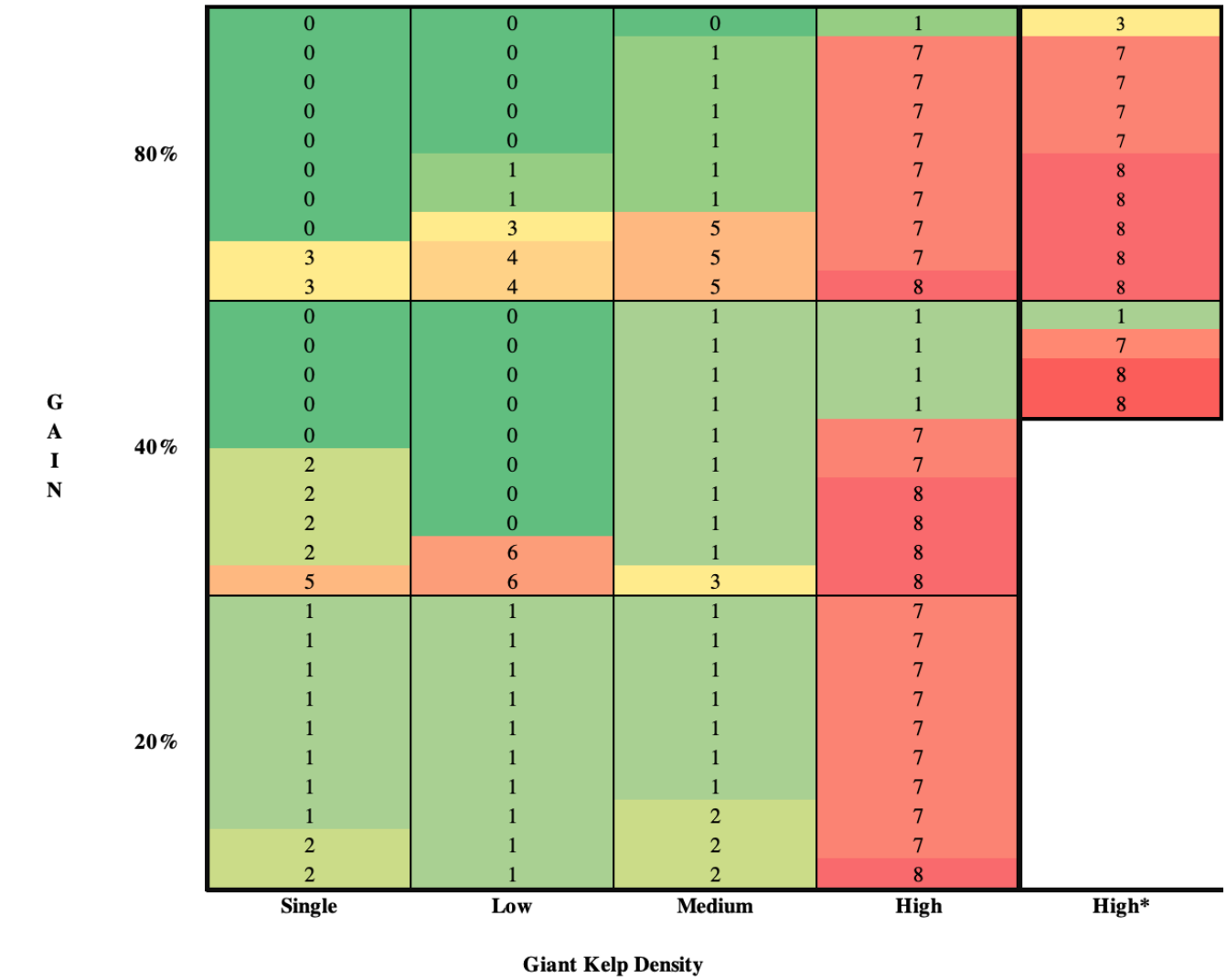

0	NE	No entanglement
1	S/NE	Slowed down, but not entangled
2	S/PE	Slowed down, entangled (with propeller), but resolved and kept moving
3	S/PE/R	Slowed down, entangled (with propeller) and ripped giant kelp blade, but pulled through
4	BE/D	Entangled (with vehicle body) but kept moving, dragging the plate
5	BE/D/K	Entangled (with vehicle body) but kept moving, dragging the plate before coming to all stop
6	BE/K	Entangled (with vehicle body) and killed, vehicle came to all stop
7	BK/NE	Blocked, not entangled
8	BK/PE	Blocked, kelp blade reached and started to wrap around propeller

Figure 4.3. Results for Restricted Movement Runs with Giant Kelp. There were nine different resulting interactions, as seen in the legend. A larger number indicates higher vegetation impact on vehicle's movement.

Single Giant Kelp

For the single giant kelp density and highest vehicle speed (80% gain) the UUV was able to go through the vegetation seamlessly 80% of the time, and 20% of the time a giant kelp blade entangled within one of the vehicle's propellers and was ripped from its blade-gas bladder connection before the vehicle could move past the vegetation. The operating region for medium speed (40% gain) and single giant kelp density showed no entanglement in 50% of the runs, while 40% of the runs resulted in giant kelp blade entanglement with at least one of the vehicle's propellers and slowing down the vehicle. In this operating region the synthetic giant kelp strand got caught up within the vehicle's body and the vehicle was able to drag the vegetation configuration plate before coming to an all stop on one occasion. All of the experimental runs at low speed (20% gain) showed a reduction of vehicle speed once it encountered the giant kelp strand, 20% of which resulted in propeller entanglement (with giant kelp blade) that resolved with the propeller eventually untangling, and 80% of them only slowed down and were not entangled.

Low-Density Giant Kelp

The only region within the experimental runs which had a consistent outcome was the low density giant kelp density and low vehicle speed (20% gain). For this region the vehicle slowed down without any entanglement 100% of the time. For the medium speed (40% gain) the vehicle was able to go through the synthetic vegetation without slowing down or entangling 80% of the time. The other 20% the vehicle's body got entangled with the giant kelp, causing it to completely stop. For the high speed runs (80% gain), 50% of the time the vehicle was able to go through without any issue, 20% of the time it slowed down while it was running over the vegetation. during one of the ten runs (10%), a giant kelp blade got entangled with the propeller and was ripped off. This interaction caused noticeable speed reduction on the vehicle. On the remaining 20% of the runs, the giant kelp got entangled with the vehicle's body. The vehicle kept moving, with the entangled giant kelp strands, dragging the plate with it.

Medium-Density Giant Kelp

For the medium density giant kelp runs and high vehicle speed (80% gain), the most common interaction is a vehicle speed reduction, without signs of any entanglement, which was seen 60% of the time. The vehicle's body got entangled with the giant kelp in a way that it kept moving, dragging the plate 30% of the time. On one occasion the vehicle was able to go through the vegetation without any apparent issues or interaction. For the medium speed (40% gain), 90% of the time the vehicle slowed down while running over the vegetation without any signs of a negative interaction such as entanglement. For the remaining run a giant kelp blade reached and entangled with a propeller, but got ripped off, allowing the vehicle to continue to move through the tank. For the slow speed runs (20% gain) the vehicle

slowed down while running over the vegetation, but there was no entanglement 70% of the time. The other 30% of the time the vehicle slowed down and had propeller entanglement that resolved by itself.

High-Density Giant Kelp

The BlueROV2 never made it into the vegetation for the low speed runs (20% gain). On one occasion (10%), even though the vehicle did not get into the vegetation, a giant kelp blade reached one of the vehicle's propeller and started to wrap around it. The remaining 90% of the runs the vehicle was stopped at the entrance of the vegetation density and was not able to get through a single strand or row. For the medium speed runs (40% gain), the BlueROV2 initially slowed down while running over the vegetation, but made it through on 40% of the runs. On two occasions the vehicle started to enter the vegetation but was blocked by it and was unable to go through its entirety. The remaining 40% of the runs had a similar outcome than the one just described, except that on these runs at least one giant kelp blade was entangled in one or more of the vehicle's propellers. For the high speed runs (80% gain), the vehicle was initially able to run over the vegetation only once (10%) while slowing down. The majority of these runs resulted in the vehicle partially running over the giant kelp vegetation before being blocked by it and coming to a complete stop. On one of these (10%) runs, one or more giant kelp blades started to wrap around a propeller, and the remaining 80% was just blocked and killed (vehicle came to an all stop).

Because it was unexpected that the vehicle was more successful at going through the vegetation density at medium speed (40% gain) than at high speed (80% gain), additional runs were performed on these two regions using the Senix probe to record the position of the vehicle over time. By recording the position and time data, the speed of the vehicle when entering the marine vegetation could be determined as well as the decrease of speed through the vegetation. This also allowed direct comparison between the runs to find any inconsistencies that might exist between them. These additional results are shown in the last column of Figure 4.3, denoted by the asterisk. For the medium speed runs (40% gain) only four extra runs were required to obtain the different interactions previously seen. From these additional four runs performed, on one occasion the vehicle slowed down while running over the vegetation, but was not entangled. On another occasion the vehicle was blocked, but not entangled, and the last two the vehicle was blocked, but with at least one giant kelp blade wrapping around one or more of the vehicle's propellers. Combining these medium speed runs with the earlier ones resulted in 35.71% slowed down without entanglement, 21.43% blocked without entanglement and 42.86% blocked with propeller entanglement. For the high speed runs (80% gain), all ten runs were repeated to confirm that only 10% of the time the vehicle was able to go through the vegetation. Although the vehicle was able to go through the vegetation only once (10%), the interaction was different. This time the vehicle slowed down, a giant kelp reached one of the propellers and

was ripped, but the vehicle continued to move through the vegetation. The BlueROV2 was blocked without any entanglement 40% of these runs and blocked with giant kelp blade and propeller entanglement 50% of the time. Combining the high speed runs resulted in vehicle slowing down without entanglement 5% of the time, vehicle slowing down with propeller entanglement and blade ripped 5% of the time, blockage without entanglement 60% of the time and blockage with propeller entanglement 30% of the time.

Figure 4.4 shows two representative vehicle position time histories for each of the two gain settings for a total of four data runs. For each gain setting, one of the runs shows the vehicle being able to go through the vegetation and the other run shows the vehicle getting blocked. The runs with a gain setting of 40% each had an average speed of 0.60 m/s (2 ft/s) and those at 80% gain each had an average speed of 1 m/s (3.3 ft/s). There was no significant difference between the vehicle's speed just prior to entering the vegetation that could be responsible for the different outcomes.

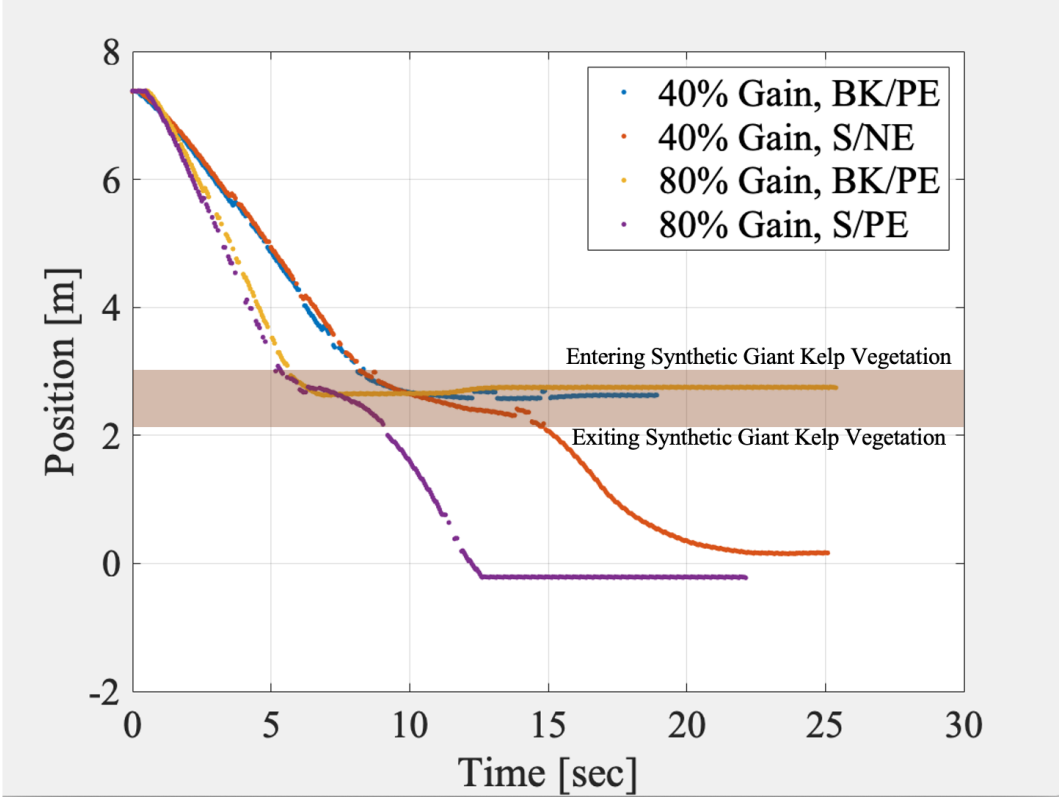

Figure 4.4. Sample data for high density giant kelp runs at 40% and 80% gain. There was no significant difference between the vegetation entry speeds that could help determine the reason why some runs were successful while others were not.

The different outcomes could be related to subtle differences in the actual location of giant kelp strands and blades with respect to the BlueROV2 since only the bottom anchor point was fixed. Even though 90% of the runs at high speed (80% gain) resulted in the vehicle being blocked by the giant kelp, the vehicle was able to go through more vegetation than the blocked runs at medium speed (40%). In all cases that the vehicle was able to go through the high density giant kelp vegetation, the vehicle slowed down to a speed close to zero prior to continuing running over the vegetation.

4.2 Synthetic Eelgrass Interactions

The interactions between the BlueROV2 and the synthetic eelgrass vegetation densities were similar to the ones presented in the previous torpedo-shaped UUV work. There were no instances of vegetation entanglement with the vehicle's body or of blockage, since the eelgrass strands are more uniform (only thin blades, no stripe, no gas bladders) and less rigid than the synthetic giant kelp strands. Because of this, there was no need to get position information during any of the runs. The many thin blades were easily pulled into to the moving propellers, shown in Figure 4.5(a), and could fit into the clearances between the propeller and the encapsulated motor, shown in Figure 4.5(b). This made it very difficult to untangle the eelgrass and required on many occasions for the eelgrass strands to be severed from the rest of the strand and the thruster to be disassembled in order to remove them, as seen in Figure 4.5(c). Figure 4.6(c) shows a pile of these severed eelgrass strands. This was a very lengthy process, since in many occasions the entanglement happened on multiple propellers and sometimes it was not visible from the outside but there were eelgrass strands inside. The severity of the damage caused on the eelgrass strands, shown in Figure 4.6, and the time it took to clear it were a driving factor when deciding not to do as many runs. On most occasions the vegetation density configuration plate had to be removed from the tank and the eelgrass strands were replaced with other strands that did not have significant plastic deformation, cut or missing strands. Examples of those types of damages to the eelgrass strands are shown in Figure 4.6(a) and 4.6(b). The limited inventory of eelgrass strands available was also a driving factor when deciding to limit the experimental runs with synthetic eelgrass.

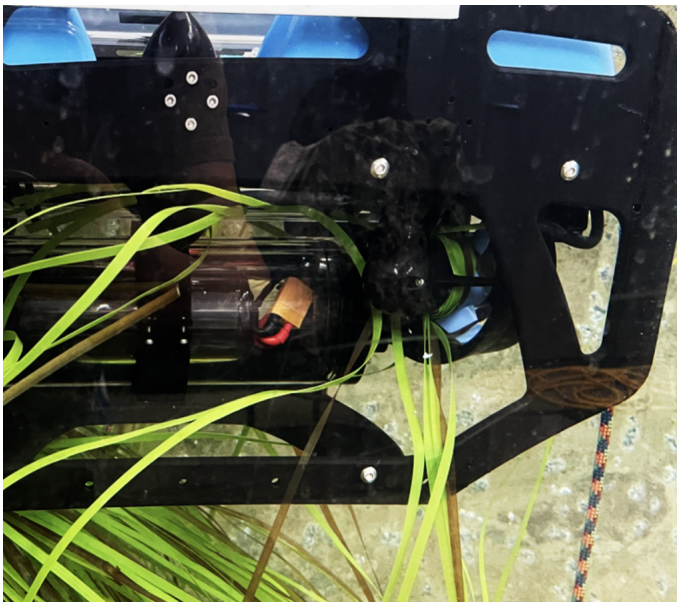

(a) Experiment Run Resulting in Eelgrass Entanglement.

(b) Eelgrass Entangled on Thruster. (c) Eelgrass Coiled on Opened Thruster.

Figure 4.5. Samples of Severe Eelgrass Entanglement with BlueROV2.

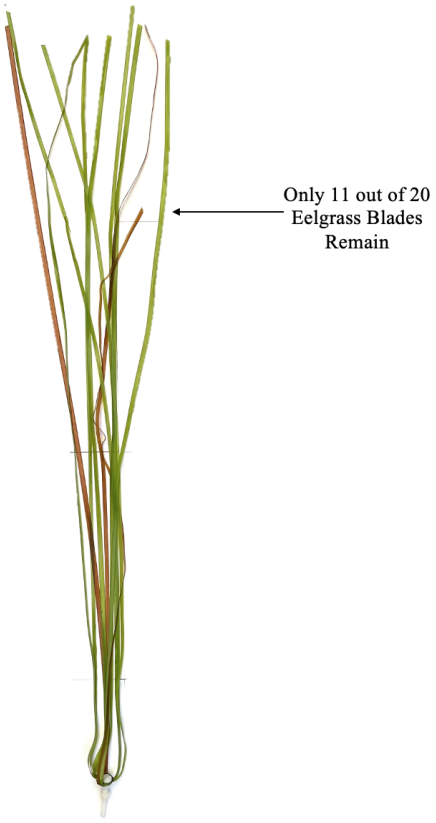

(a) Damaged Eelgrass Strand.

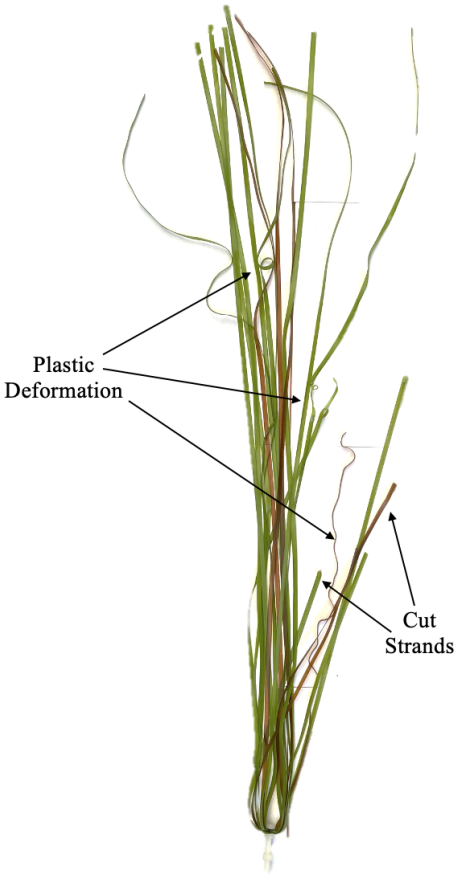

(b) Damaged Eelgrass Strand.

(c) Pile of Damaged Eelgrass.

Figure 4.6. Samples of Damaged Eelgrass.

4.2.1 Unrestricted Movement Runs

For the unrestricted runs done without the test fixture and using the depth hold mode, only the speed achieved with a 50% gain setting was tested in both forward and astern operations. Only two different interactions resulted from these runs. The two interactions were either no entanglement, or entanglement that resulted in the vehicle not being able to move past the vegetation density.

For these runs, only one of the six runs made it through the single eelgrass strand without getting entangled and stuck. This was one of the three astern operation runs. The remaining runs resulted in severe entanglement of the vehicle with the single eelgrass strand, all of the forward operation runs and two of the three astern operation runs.

4.2.2 Restricted Movement Runs

Only forward operation restrict motion runs were conducted. A total of five different interactions resulted from these experimental runs, as shown on Figure 4.7. The lowest interaction, labeled with the number zero is the same one defined previously for the giant kelp tests. In this case the vehicle is able to go past the vegetation without any issues or significant reduction in speed. The interaction labeled with the number one was used whenever there was entanglement with the propeller but the vehicle was going at a fast enough speed that the propeller ripped the eelgrass blade without there being any significant changes on the vehicle's speed. The next interaction, labeled with the number two, was used whenever the eelgrass entangled with one or more of the vehicle's propellers and slowed down the vehicle but the propeller eventually became untangled and the vehicle was able to go past the vegetation. The interaction that follows this, labeled with the number three, was similar to the last two. The eelgrass would reach the propellers, the vehicle would slow down, the eelgrass was ripped from the strand(s) and the vehicle would complete the run. The highest level of interaction, labeled with the number four, was when the vehicle would slow down due to propeller entanglement with the eelgrass and was not able to move forward anymore. On these cases the level of entanglement, both the number of propellers entangled and the number of eelgrass blades entangled per propeller, was so severe that a significant number of eelgrass blades had to be severed in order to free the vehicle. As the number of runs resulting in a level four interaction grew, the synthetic eelgrass inventory had less and less blades per strand, and fewer runs were conducted when this was the expected result.

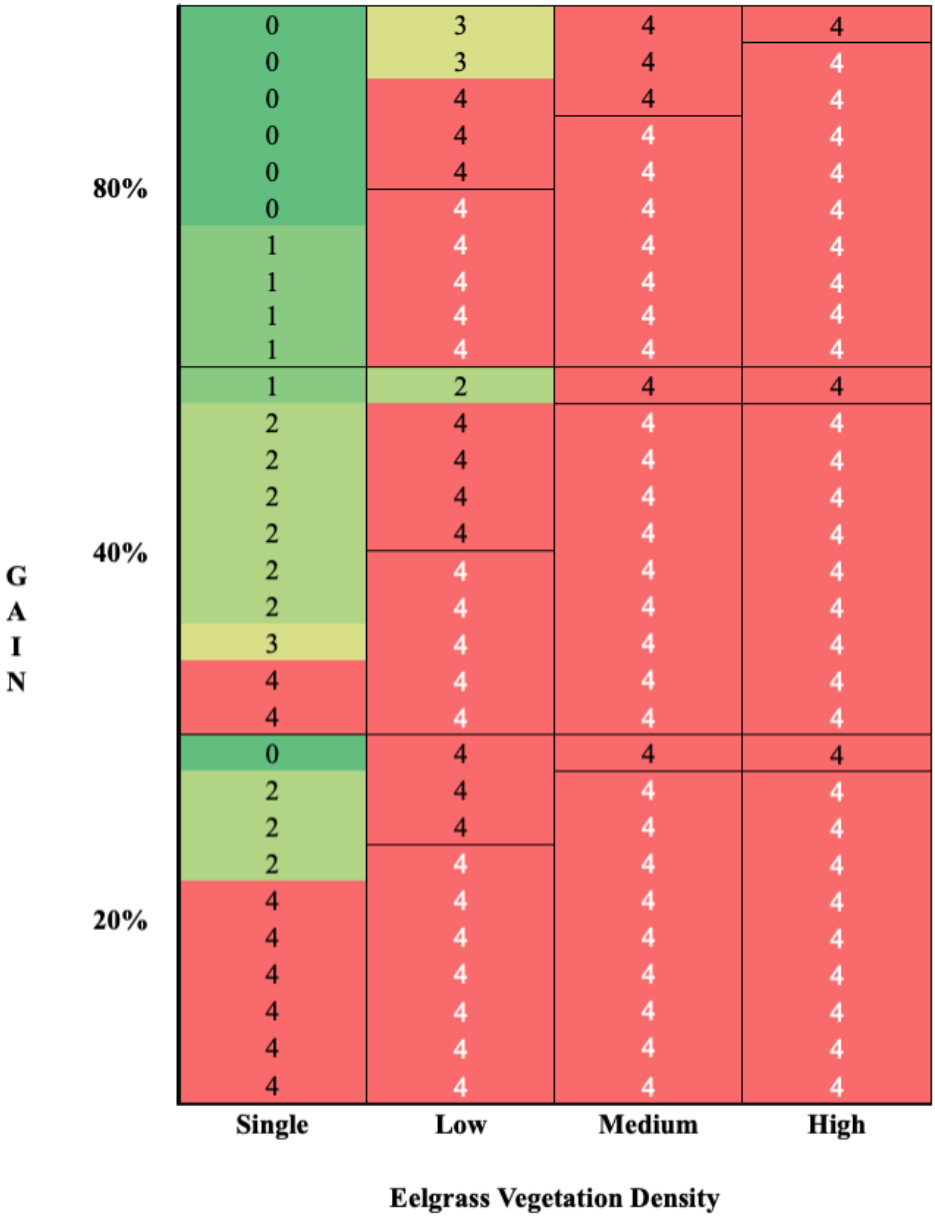

0	NE	No entanglement
1	PE/R/NS	Entangled (with propeller) and ripped but no significant speed change (not slowed down)
2	S/PE	Slowed down due to entanglement (with propeller), but resolved and kept moving
3	S/PE/R	Slowed down due to entanglement (with propeller) ripped eelgrass blade, kept moving
4	S/PE/K	Slowed down due to entanglement (with propeller), vehicle came to all stop
4	S/PE/K*	Expected outcome: slow down due to propeller entanglement and coming to an all stop

Figure 4.7. Results for Experimental Runs with Eelgrass. There were four different resulting interactions, as seen in the legend. Larger number indicate higher vegetation impact on vehicle's movement.

Ten runs were performed for the single eelgrass vegetation density for the high speed setting (80% gain), medium speed setting (40% gain) and low speed setting (20% gain). For the low eelgrass vegetation density only five runs were conducted for the high speed setting (80% gain) and the medium speed setting (40% gain), and three runs for the low speed setting (20%). Because of the consistency of the results, fewer repeat runs were conducted. For the medium eelgrass vegetation density only three runs were conducted for the high speed setting (80% gain), and one for the medium (40% gain) and low (20% gain) speed settings. If the runs at a given eelgrass density and high speed resulted in entanglement, it was assumed that runs at the same eelgrass density and lower vehicle speeds would also entangle. This is because entanglement was more likely to occur at lower speeds, since the vehicle spent more time in the vegetation area. At least one run was still conducted to confirm this assumption. For the high eelgrass density, one run was conducted for each of the selected speed settings (80%, 40% and 20% gain). If the runs at a lower eelgrass density and a given speed resulted in entanglement, it was assumed that entanglement would also occur at the same speed and higher eelgrass density. Higher eelgrass density would mean more entanglement opportunities due to more eelgrass blades; however, one run was still conducted to confirm assumptions.

Single Eelgrass Vegetation

The single eelgrass vegetation density and high speed setting (80% gain) was the operating region with the best prognosis. In this region the vehicle was able to move past the vegetation without any issues 60% of the time, and the other 40% of the time eelgrass blades would reach the propeller, but the propeller was spinning fast enough to rip the blades almost instantaneously without significantly slowing down the vehicle. In the majority of the runs (60%) conducted at the medium speed setting (40% gain), the vehicle slowed down due to propeller entanglement that resolved and the vehicle was able to go past the vegetation. On one occasion (10%) the entangled eelgrass was ripped and the vehicle kept moving without any significant speed changes. On another occasion (10%) the entangled eelgrass was ripped, but there was a significant vehicle speed reduction noticed. The remaining 20% of the runs the vehicle was entangled until it came to an all stop (kill). For the low speed runs (20% gain setting) the vehicle was able to go through the eelgrass strand without any issues on one occasion (10%). The majority of the time (60%) the vehicle would entangle in such a way that it came to an all stop (kill). The remaining three runs (30%) resulted on eelgrass entangled, blades ripped, and the vehicle slowing down, but it kept moving past the vegetation.

Low-Density Eelgrass

The majority of the runs using the low eelgrass vegetation density resulted in vehicle entanglement and subsequent kill. For the high speed runs (80% gain setting) this was the

case for three of five runs. The other two runs resulted in entangled and ripped eelgrass that slowed down but did not precluded the runs. For the medium speed runs (40% gain setting) entanglement and kill happened four of the five runs. The remaining run resulted in eelgrass entanglement that slowed down the vehicle but resolved on its own. All of the runs conducted at low speed (20% gain setting) resulted in the vehicle slowing down due to entanglement of eelgrass blades with the vehicle's propeller and the vehicle coming to an all stop (kill). The remaining runs for each of the different speed regions that were not conducted were expected to result in the most severe interaction. This is shown on Figure 4.7 with a white number four and a red background.

Medium-Density and High-Density Eelgrass

The entirety of the runs conducted on both the medium and the high eelgrass vegetation density resulted in the vehicle slowing down due to the entanglement of eelgrass blades with multiple propellers of the vehicle, and the vehicle coming to an all stop (kill). As mentioned previously in Section 4.2.1, only three runs were conducted on the medium eelgrass vegetation density with the vehicle in the high speed setting (80% gain) and one for each medium (40% gain) and low (20% gain) speed settings. Section 4.2.1 also mentions that only three runs were conducted for the high eelgrass vegetation density, one per vehicle speed setting (80%, 40% and 20% gain). A white number four on a red background is again used to represent the expected results if the full ten runs were conducted.

4.3 Effects of Vehicle Geometry on Results

Because the same facility and vegetation, along with similar procedures, were used for the previous work with a REMUS100, which is an 355.86 N (80-pound) torpedo-shaped UUV, a direct comparison can be made between those results and the results of this investigation. Table 4.1 compares the speeds used for this thesis and in the previous work for low (L), medium (M) and high (H) settings. The speed settings for this thesis were chosen to be as close as possible to the previous work to allow direct comparison; however, the BlueROV2 was not able to move the carriage at a gain setting below 20%. Note that the data compared are three runs that were performed for the REMUS100 runs.

Table 4.1. REMUS100 and BlueROV2 Speed Comparison. Adapted from: [20], [21].

Speed	REMUS100 (m/s)	BlueROV2 (m/s)	% Difference
L	0.17	0.25	19%
M	0.62	0.61	1%
H	0.94	1.00	3%

4.3.1 Synthetic Giant Kelp Interactions

Figure 4.8 displays the results in percentages for both the REMUS100 and the BlueROV2 for the experimental runs with different giant kelp vegetation densities and vehicle speed runs. The giant kelp had no effect on the operation of the REMUS100, but it significantly affected the BlueROV2, even at the single giant kelp density. The resulting BlueROV2 interactions with the synthetic giant kelp were simplified in order to compare with the REMUS100's results, tying the outcome to one of six possibilities. If there was no interaction, the letter "N" was assigned to it. If the vehicle slowed down while going over the vegetation, and was not entangled or blocked, the letter "S" was assigned to it. If there was any entanglement with the vehicle's body, the letters "BE" were assigned to it. Runs resulting in propeller entanglement were assigned "PE", unless that propeller entanglement prevented the vehicle from moving any further. In that case the letter "K" was assigned to it. Finally, if the vehicle was blocked by the synthetic giant kelp, the letter "B" was used to describe the outcome.

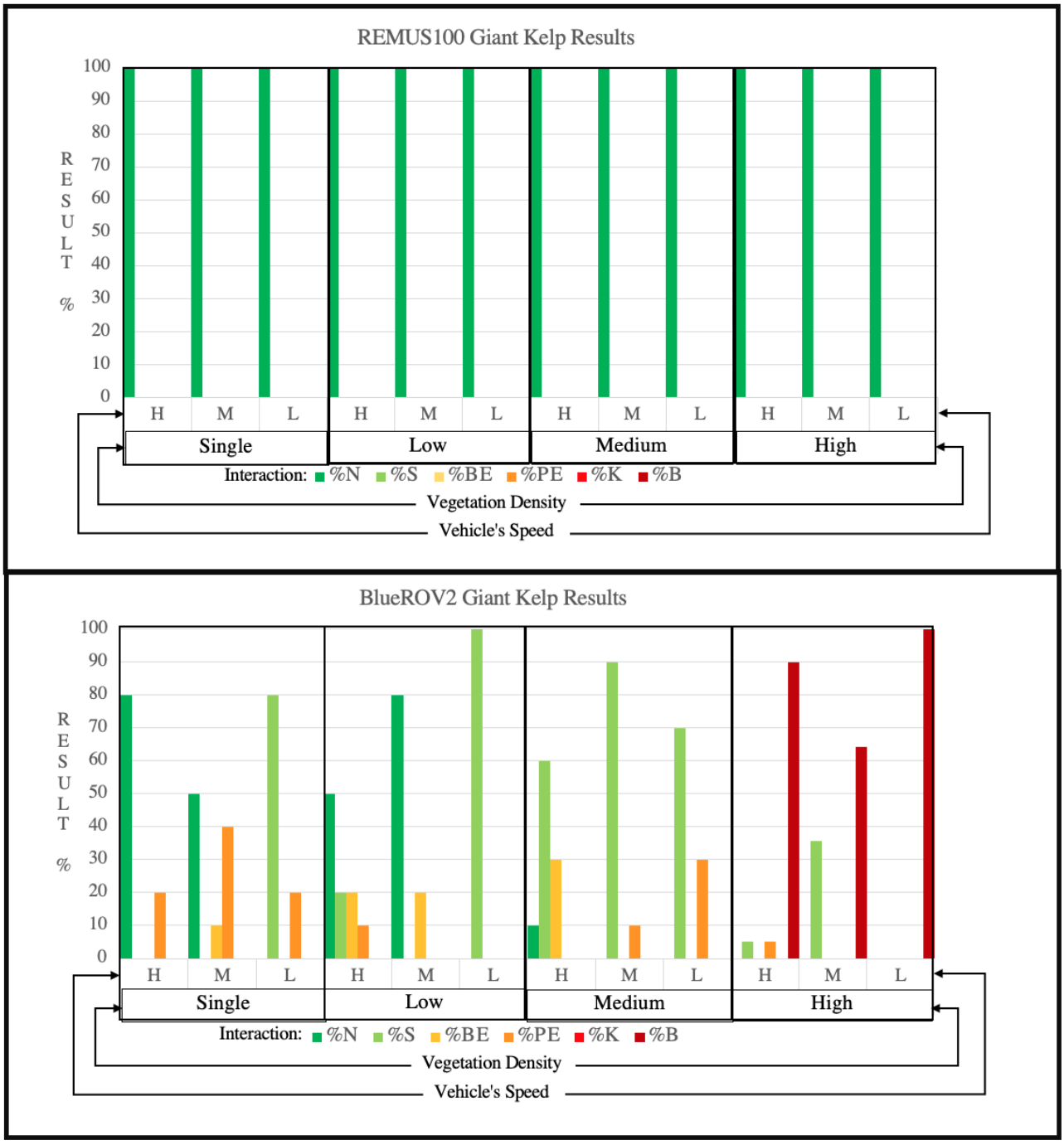

Figure 4.8. REMUS100 and BlueROV2 Giant Kelp Results. The synthetic giant kelp had no effect on the REMUS100's operation, while it showed a wide range of interactions with the BlueROV2. Adapted from: [20], [21].

The BlueROV2's segmented and boxy geometry, as well as its much lower weight (about 70% lighter) was likely to blame. The thicker portions of the synthetic giant kelp strand, such as the gas bladders and the stripe, entangled on the clearances between the UUV's components. By having a lower mass, the BlueROV2 has lower momentum and kinetic energy, putting it at a disadvantage. Its relatively large width (0.34 m or 13.3 in) when compared to the REMUS100's diameter (0.19 m or 7.5 in) would have also provided additional contact areas with the vegetation. This also made it more difficult for the BlueROV2 to push away the vegetation and required for the vehicle to run over it.

4.3.2 Synthetic Eelgrass Interactions

The results of the BlueROV2 runs with the synthetic eelgrass yielded similar interactions to that of the REMUS100 vehicle. Because the synthetic eelgrass is not as rigid as the giant kelp, there were no instances of entanglement with the BlueROV2's body. Figure 4.9 displays the results in percentages for both the REMUS100 and the BlueROV2 for the experimental runs with different eelgrass vegetation densities and vehicle speed runs. Similar to what was done in the previous section, the eelgrass interactions with the BlueROV2 were simplified to allow better comparison. The letter "N" was still used whenever there was no significant interaction between the vehicle and the vegetation. If the runs resulted in propeller entanglement, the letters "PE" were assigned to it, unless that propeller entanglement prevented the vehicle from moving any further. In that case the letter "K" was used to describe the resulting interaction.

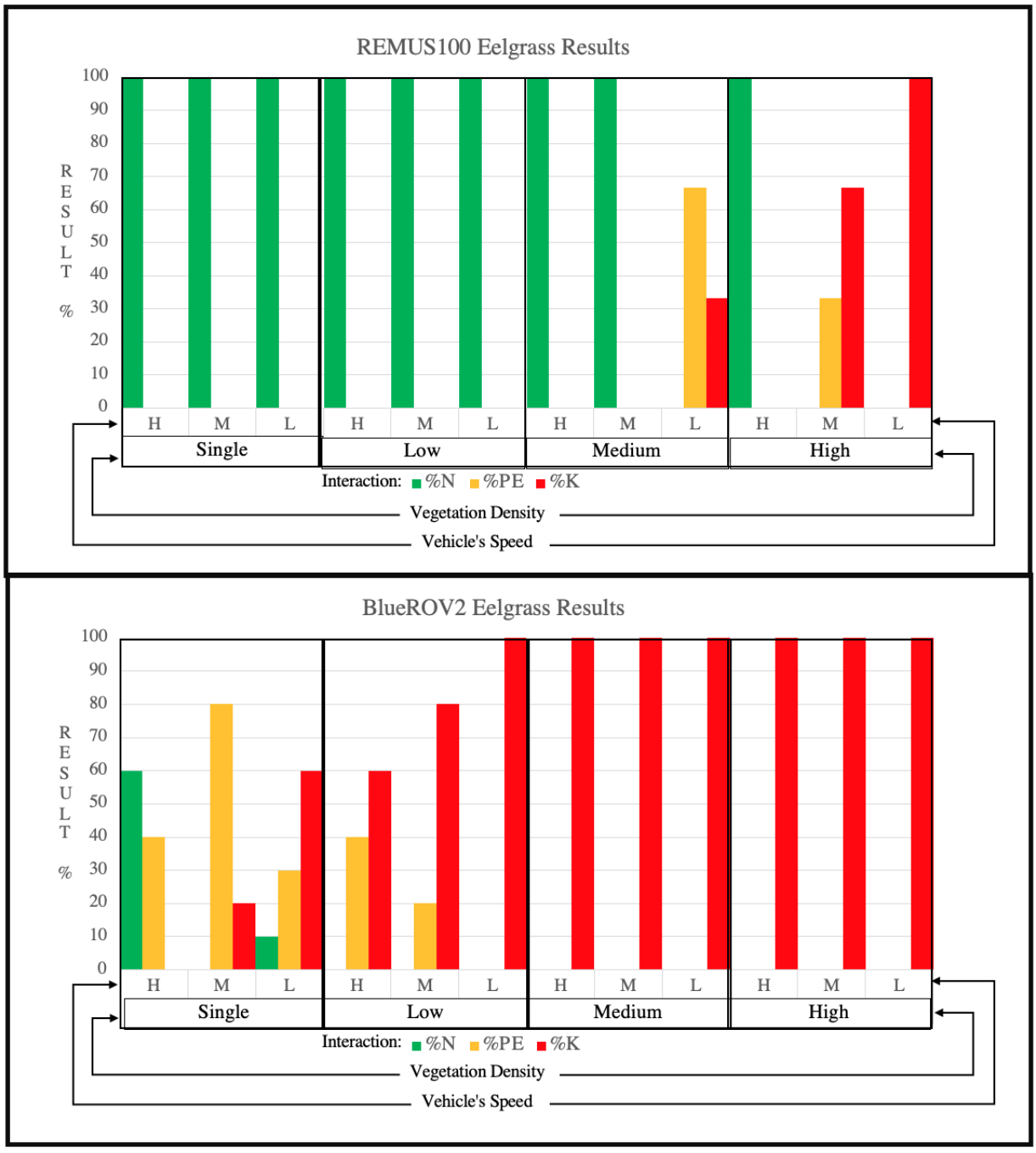

Figure 4.9. REMUS100 and BlueROV2 Eelgrass Results. The synthetic eelgrass only negatively affected the REMUS100's operation at medium and high densities. The BlueROV2 had negative interactions even with the single eelgrass density. Adapted from: [20], [21].

The REMUS100 was not affected by the eelgrass whenever the single or low vegetation configurations were used. For the medium eelgrass density configuration, the REMUS100 was only affected on its low speed runs. The high eelgrass density configuration had a negative effect on both the medium and low speed settings, but not on the high speed setting runs. The BlueROV2 did have some negative interactions, even with the single eelgrass vegetation density. At the low eelgrass vegetation density, the vehicle did have some instances in which the propeller entanglement ultimately resolved by itself, but all of the runs at the low eelgrass density and low vehicle speed resulted in a "K". All of the runs conducted at the medium and high eelgrass density configurations resulted on the propeller entanglement that did not resolve itself and prevented the vehicle from advancing ("K").

The severity of the interactions between the synthetic eelgrass and the BlueROV2 was likely due to its shape, number of propellers, and location of the propellers. The REMUS100 only has one propeller, and it is on the aft portion of the vehicle. This allows the forward portion of the vehicle to displace the vegetation prior to encountering the propeller. It also has aft control surfaces that also tend to push vegetation away from the propeller disk. With the BlueROV2, the eelgrass will encounter two propellers just as the vehicle starts to go through the vegetation, and four by the time the vehicle is moving through it.

CHAPTER 5:
Conclusions and Future Work

A wide range of interactions were observed, and presented in Chapter 4. These interactions were determined to be marine vegetation type and density dependent. Although similar interactions were observed between the unrestricted and restricted movement runs, the unrestricted movement runs showed more negative interactions due to higher number of thrusters operating and the vegetation's impact on the vehicles ability to maintain depth. The data collected was compared to the data that was collected from previous work, using similar procedures and equipment, but a different UUV. The results were compared to see if any conclusions could be made based on vehicle's geometry. More information is needed to better understand the implications of vehicle's size and shape, to include mass, diameter, or width on the probability of entanglement with marine vegetation. This chapter summarizes the findings from the previous chapter and lists recommendations for future work.

5.1 Conclusions

The results presented in Chapter 4 show that there are multiple factors that affect the interactions between a UUV and marine vegetation. The vegetation type and density, as well as vehicle speed are some of these factors. Vehicle movement (restricted versus unrestricted) and the implications for the number thrusters used for each type of movement are also factors. Lastly, vehicle geometry (and possibly mass) was also determined to be factors affecting the interactions between UUVs and marine vegetation.

5.1.1 Vegetation (Type and Density) and Vehicle Speed

A wide range of interactions were seen between the BlueROV2 and the marine vegetation. The runs with giant kelp showed some new interactions not previously seen, while the eelgrass runs showed the same expected interactions. As expected, higher vegetation densities generally resulted in more negative interactions when compared to lower vegetation density configurations. In general the runs conducted with faster vehicle speeds resulted in less negative interactions than those at lower vehicle speeds.

The giant kelp caused some entanglement with the vehicle's body (mostly due to gas bladders), as well as the vehicle's propellers. It was not expected that the low density giant kelp would show better outcome compared to those seen with the single giant kelp, as seen in the low speed (20% gain) and medium speed (40% gain) runs. This could possibly be due to the fact that the single giant kelp strand was directly in the vehicle's

path, while the four strands used to create the low density were not. Overall the runs at higher speeds and lower vegetation density had better probability of mission success, with the exception of high giant kelp density, which had different kind of interactions. Runs at higher giant kelp density showed the most negative interactions, completely blocking the vehicle (preventing the vehicle from entering the vegetation) at low speeds and blocking it once inside the vegetation at medium and high speeds. Due to less negative interactions between the BlueROV2 and the synthetic giant kelp on some areas at medium speeds than at high speeds, it is possible that where the different parts of the synthetic giant kelp end up within the run have a significant effect on the outcome.

The synthetic eelgrass was very flexible and thin, causing entanglement only with the propellers. There were no cases of vehicle blockage due to eelgrass vegetation. The runs with the synthetic eelgrass vegetation densities also showed better prognosis at higher vehicle speeds and lower vegetation density.

5.1.2 Vehicle Movement (Restricted vs Unrestricted)

The runs without the testing fixture confirmed that a higher number of propellers operating results in a higher probability of entanglement, as well as difficulty maintaining depth. This was true for both the giant kelp and eelgrass runs. When attempting to get through the giant kelp the vehicle changes depth which then causes additional propellers, essentially the vertical thrusters, to also start rotating. For the unrestricted runs with eelgrass, as soon as any eelgrass blade got entangled with any vehicle propeller, the vehicle was unable to maintain depth, but would try to by actuating the vertical thrusters, which resulted in more entanglement.

5.1.3 Vehicle Geometry

When comparing a single propeller (astern placement, 80-lb, torpedo-shaped) UUV with the BlueROV2 (24-lb, box-shaped, six propellers), the torpedo shaped UUV had better outcome for all of the different vegetation configurations and the selected speeds. There were significant differences between the two vehicles and the synthetic giant kelp vegetation densities. The REMUS100's operation was not affected at all by the giant kelp, while the BlueROV2 slowed down while running over it, entangled both with the propellers and the vehicle's body, and on some occasions it was blocked. The interactions between the vehicles and the synthetic eelgrass were not that dissimilar; however, the BlueROV2 had worse outcomes due to higher number of operating propellers and propeller location.

5.2 Future Work

Further testing with the BlueROV2 vehicle could be done to get information on its performance in other types of marine vegetation and vegetation densities. These experimental runs could also be repeated with different vehicles to assess different geometry and propulsion UUV options. Other parameters to be investigated would be vehicle's mass and width (or diameter).

5.2.1 Vegetation Considerations

This thesis, and prior work, focused on giant kelp and eelgrass, which are predominant on USN operating coastal waters. The use of other marine vegetation could also be explored. Another option would be testing the vehicles in a real-world setting with real marine vegetation instead of synthetic ones. This may not lead to data that could be directly compared to the one previously obtained, nor would it be repeatable, but it would confirm or disprove that the synthetic marine vegetation used was "close enough" to real vegetation, potentially validating the results presented on this thesis.

5.2.2 Vehicle Considerations

So far the only vehicles tested have been a 355.86 N (80 lb), 0.19 m (7.5 in) diameter torpedo shaped UUV and a 106.76 N (24-lb), 0.34 m (13.3 in) wide box-shaped UUV. Would the results differ if the same torpedo shaped UUV were lighter or heavier, or had a larger or smaller diameter? The same could be true for the box-shaped UUV. Would a heavier one have more successful outcomes, or a slimmer (smaller width) one? More could be investigated about the width or diameter of the UUVs relative to the characteristic length scales of the marine vegetation. For this question the same geometry and width is used while adding or removing weight from the vehicle. This would affect the vehicle's speed and therefore the tank's carriage would have to be operating in order to keep vehicle speed constant. For the width or diameter question the vehicle's geometry and weight is to be kept the same and the width is changed by adding 3D printed shells. Because the weight of the vehicle is to be kept the same throughout the experiment, the weight of the largest shell is to be compensated in the other configurations. Is the probability of mission success (going through a marine vegetation field) related to the relationship between the UUV's width (or diameter) and the spacing between the vegetation, in this case the synthetic strands?

Testing other vehicles with different geometries and propulsion methods would provide more useful information to help decide which vehicles to use for specific areas and missions. Testing vehicles with the same mass and width but different shapes, would give more clear data as to which shape is better at going through marine vegetation. For those vehicles using propellers for propulsion, how does the number of propellers affect the probability

of entanglement? Will more propellers always lead to more entanglement? Is there a relationship between the two? If so, what kind of relationship? How important is the placement (location) of the propellers?

5.2.3 Vehicle Operation Considerations

Lateral placement tests, similar to the ones conducted in the previous work should be repeated with the BlueROV2. This would aid in understanding the probability of vehicle entanglement depending on the distance between the marine vegetation and the vehicle's center. The vehicle's depth in relation to the length of the vegetation should also be considered. For these the same speed and vegetation type and density would be used, while changing the depth of the vehicle via the sting, as discussed in Section 2.2.

For UUVs propelled with thrusters, the relationship with propeller rpm, vehicle speed, and marine vegetation entanglement should be further investigated. For this experiment the vehicle's speed should be set by the tank's carriage. The vehicle's rpm should then be changed during the runs from the lowest possible setting to the highest setting. The experiment would then be repeated for different speeds. Based on the results it could be determined whether vehicle speed or propeller rpm have a higher impact on the probability of entanglement. If this is known, as well as any mass and number of operating propeller relationship, then an optimum design could be derived.

APPENDIX: Engineering Drawing of Adapter

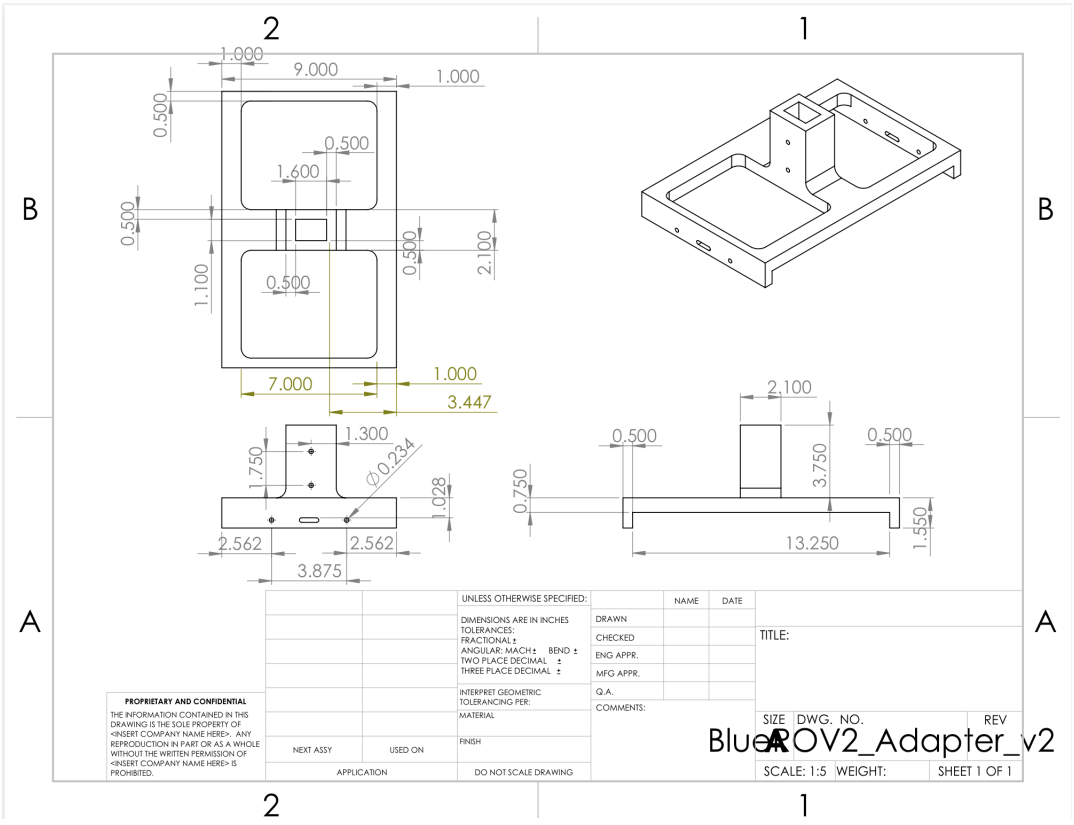

Figure A.1. Engineering Drawing of Adapter. Dimensions shown in inches.

THIS PAGE INTENTIONALLY LEFT BLANK

List of References

[1] Oceana Org. "Corals and other invertebrates: Giant kelp". Accessed Sep. 6 2021 [Online]. Available: https://oceana.org/marine-life/corals-and-other-invertebrates/giant-kelp

[2] NOAA's National Marine Sanctuaries. "Kelp forests- a description". Accessed Sep. 6 2021 [Online]. Available: https://sanctuaries.noaa.gov/visit/ecosystems/kelpdesc.html

[3] Great Ocean Road Coast Committee. (2011, March). "An underwater world in decline". [Online]. Available: https://gorcc.org/tag/giant-kelp/

[4] Richardson Bay Audubon Center & Sanctuary. "Conversation - All about eelgrass". Accessed Feb. 13, 2021 [Online]. Available: https://richardsonbay.audubon.org/conversation/all-about-eelgrass

[5] F. Short, T. Carruthers, M. Waycott, G. Kendrick, J.W.Fourqurean, A. Callabine, W. Kenworthy, and W. Dennison, "Zostera marina the IUCN red list of threatened species," International Union for Conservation of Nature and Natural Resources, UK, Tech. Rep. e.T153538A4516675, Oct. 2010. Available: https://dx.doi.org/10.2305/IUCN.UK.2010-3.RLTS.T153538A4516675.en

[6] U.S. 6th Fleet. "About us - Area of responsibility". Accessed November 2, 2021 [Online]. Available: https://www.c6f.navy.mil/About-Us/

[7] M. Breivik and T. Fossen, "Guidance laws for autonomous underwater vehicles," *Underwater Vehicles*, doi:10.5772/6696. isbn:978-953-7619-49-7 Jan. 2009.

[8] Bluebird Marine Systems Limited. "ROVs - UUVs - USVs & drones". Accessed October 16, 2021 [Online]. Available: https://www.bluebird-electric.net/ROV_remotely_operated_vessels_UUV_underwater_unmanned_autonomous_drones.htm

[9] D. Trekker. "Top 3 uses for mini-ROVs in the Navy". Accessed October 16, 2021 [Online]. Available: https://www.deeptrekker.com/resources/top-3-uses-for-mini-rovs-in-the-navy

[10] Naval Sea Systems Command (NAVSEA). "Remotely operated vehicles". Accessed October 16, 2021 [Online]. Available: https://www.navsea.navy.mil/Home/SUPSALV/00C2-Salvage/Remotely-Operated-Vehicles/

[11] P. Small, “Unmanned maritime systems update,” https://www.navsea.navy.mil/Portals/103/Documents/Exhibits/SNA2019/Unmanned-MaritimeSysSmall.pdf?ver=2019-01-15-165105-297, January 2019.

[12] R. Wernli, “AUV commercialization-who’s leading the pack?” in *OCEANS MTS/IEEE Conf. and Exhi.*, Sep. 2000, vol. 1, pp. 391 – 395 vol.1. Available: doi:10.1109/OCEANS.2000.881290

[13] T. Curley. "Hybrid AUV/ROV: A multi-mission vehicle transforming underwater exploration and inspection". Accessed October 16, 2021 [Online]. Available: http://digital.ecomagazine.com/publication/?i=482821&article_id=3038191&view=articleBrowser&ver=html5

[14] Blue Robotics Inc. "BlueROV2". Accessed July 12, 2021 [Online]. Available: https://bluerobotics.com/store/rov/bluerov2/

[15] M. Purcell, C. von Alt, B. Allen, T. Austin, N. Forrester, R. Goldsborough, and R. Stokey, “New capabilities of the remus autonomous underwater vehicle,” in *OCEANS 2000 MTS/IEEE Conference and Exhibition. Conference Proceedings (Cat. No.00CH37158)*, 2000, vol. 1, pp. 147–151 vol.1.

[16] Woods Hole Oceanographic Institution. "REMUS 100". Accessed Feb. 16, 2021 [Online]. Available: https://www2.whoi.edu/site/osl/vehicles/remus-100/

[17] P. Kodati and X. Deng, “Bio-inspired robotic fish with multiple fins,” in *Underwater Vehicles*, A. V. Inzartsev, Ed. Rijeka: IntechOpen, 2009, ch. 6. Available: https://doi.org/10.5772/6698

[18] M. Ball. (2015, September). Boston Engineering Receives Grant to Commercialize BIOSwimmer UUV. UST. [Online]. Available: https://www.unmannedsystemstechnology.com/2015/09/boston-engineering-receives-grant-to-commercialize-bioswimmer-uuv/

[19] S. Wasserman. (2019, Aug 19). Engineers Use Biomimicry to Innovate the Propulsion of Unmanned Underwater Vehicles. ANSYS. [Online]. Available: https://www.ansys.com/blog/biomimicry-innovates-unmanned-underwater-vehicles

[20] K. Irgens, “Experimental assessment of entanglement for unmanned underwater vehicle with an open three-bladed propeller,” M.S. thesis, Naval Postgraduate School, Monterey, CA U.S.A., 2020.

[21] K. Irgens, J. Klamo, and A. Pollman, “Experimental assessment of entanglement for a propeller driven unmanned underwater vehicle,” *Naval Engineers Journal*, vol. 133, no. 3, 2021.

[22] DroneCode Project Inc. (2019). "QGROUNDCONTROL - Intuitive and powerful ground control station for the MAVLink protocol.". [Online]. Available: http://qgroundcontrol.com/

[23] Blue Robotics Inc. "BlueROV2 operation". Accessed September 14, 2021 [Online]. Available: https://bluerobotics.com/learn/bluerov2-operation/

[24] Bio Models Co. (2009). "Bio Models Company - Who we are". [Online]. Available: https://biomodelscompany.com/who-we-are/

[25] Bio Models Co. "Plant characteristics". Accessed September 13, 2021 [Online]. Available: https://biomodelscompany.com/plant-characteristics-2/

THIS PAGE INTENTIONALLY LEFT BLANK

Initial Distribution List

1. Defense Technical Information Center
   Ft. Belvoir, Virginia

2. Dudley Knox Library
   Naval Postgraduate School
   Monterey, California